Supplementary Material

Novel oxaliplatin (IV) complexes conjugated with ligands bearing pendant 1,2-dithiolane/1,2-diselenolane/cyclopentyl motifs

Xiao Liu[a] +, Dominik Wenisch[b] +, Marie-Christin Barth[a], Klaudia Cseh[b], Christian R. Kowol[b], Michael A. Jakupec[b], Dan Gibson[c]*, Bernhard K. Keppler[b]*, Wolfgang Weigand[a]*

[a] *Xiao Liu, Marie-Christin Barth, Prof. Dr. Wolfgang Weigand*
Institute for Inorganic and Analytical Chemistry,
Friedrich Schiller Universität Jena,
Humboldt Str. 8, 07743 Jena, Germany.
E-mail: wolfgang.weigand@uni-jena.de

[b] *Dominik Wenisch, Klaudia Cseh, Assoc. Prof. Dr. Christian R. Kowol, Dr. Michael A. Jakupec, Prof. Dr. Dr. Bernhard K. Keppler*
Institute of Inorganic Chemistry, Faculty of Chemistry,
University of Vienna,
Währinger Strasse 42, 1090 Vienna, Austria
Email: bernhard.keppler@univie.ac.at

[c] *Prof. Dr. Dan Gibson*
Institute for Drug Research, School of Pharmacy,
The Hebrew University of Jerusalem,
Jerusalem, 91120 (Israel)
E-mail: dang@ekmd.huji.ac.il

[+] These authors contributed equally to this work.

Table of Contents

Part 1. Supplementary figures and schemes

Part 2. NMR spectra

Part 3. MS spectra

Part 4. Concentration-effect curves

Part 1. Supplementary figures and schemes

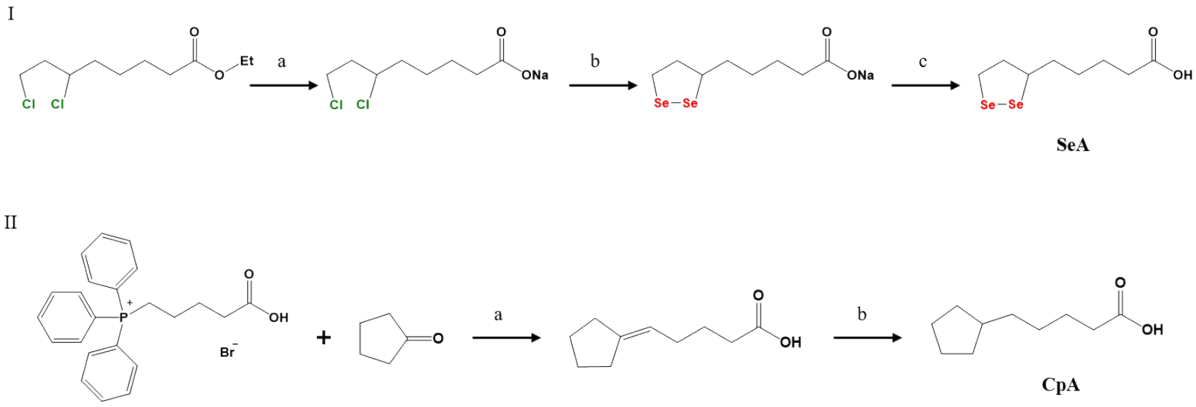

Scheme S1. The systhesis route of ligands SeA and CpA. Reactants and conditions:(I) a: NaOH/H_2O-EtOH; 50 ℃, 1.5 h; b: Na_2Se_2/H_2O-EtOH; 65 ℃, 2 h; c: aq. HCl; 0 ℃. (II) a: $KNSi_2(CH_3)_6$/anhydrous THF; reflux, 24h; b: H_2, 10% Pd/C,5% mol/DCM; r.t. 2days.

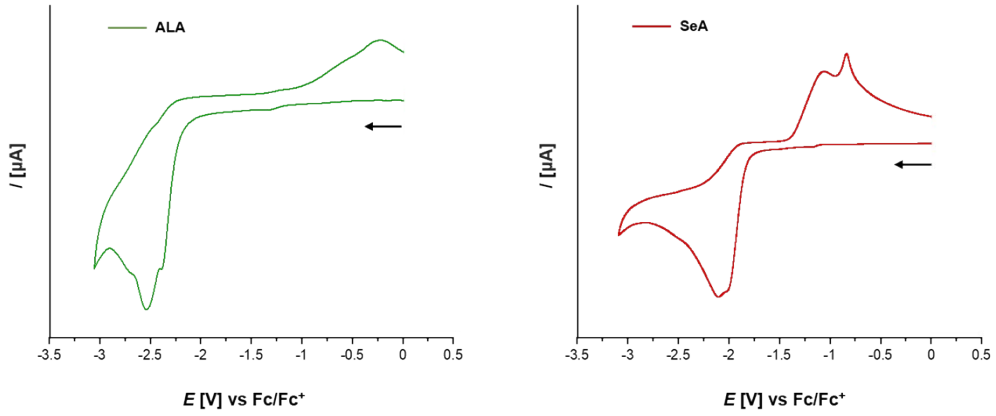

Figure S 1. The cyclic voltammograms of 1 mM ALA and SeA in 0.1 M DMF- [n-Bu_4N][PF_6] at a scan rate of 0.2 Vs^{-1}

(a)

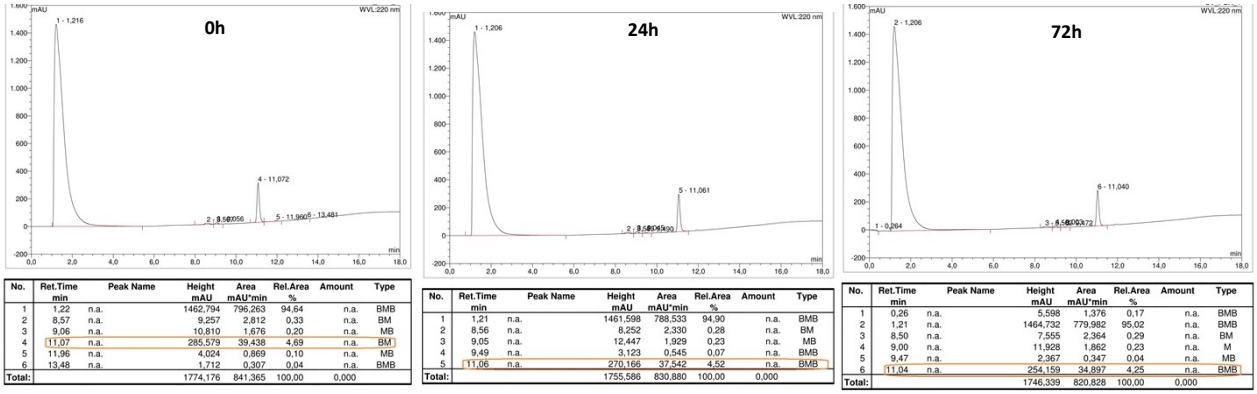

No.	Ret.Time min	Peak Name	Height mAU	Area mAU*min	Rel.Area %	Amount	Type
1	1,22	n.a.	1462,794	796,263	94,64	n.a.	BMB
2	8,57	n.a.	9,257	2,812	0,33	n.a.	BM
3	9,06	n.a.	10,810	1,676	0,20	n.a.	MB
4	11,07	n.a.	285,579	39,438	4,69	n.a.	BM
5	11,96	n.a.	4,024	0,869	0,10	n.a.	MB
6	13,48	n.a.	1,712	0,307	0,04	n.a.	BMB
Total:			1774,176	841,365	100,00	0,000	

No.	Ret.Time min	Peak Name	Height mAU	Area mAU*min	Rel.Area %	Amount	Type
1	1,21	n.a.	1461,598	788,533	94,90	n.a.	BMB
2	8,56	n.a.	8,252	2,330	0,28	n.a.	BM
3	9,05	n.a.	12,447	1,929	0,23	n.a.	MB
4	9,49	n.a.	3,123	0,545	0,07	n.a.	BMB
5	11,06	n.a.	270,166	37,542	4,52	n.a.	BMB
Total:			1755,586	830,880	100,00	0,000	

No.	Ret.Time min	Peak Name	Height mAU	Area mAU*min	Rel.Area %	Amount	Type
1	0,26	n.a.	5,598	1,376	0,17	n.a.	BMB
2	1,21	n.a.	1464,732	779,982	95,02	n.a.	BMB
3	8,50	n.a.	7,555	2,364	0,29	n.a.	BM
4	9,00	n.a.	11,928	1,862	0,23	n.a.	M
5	9,47	n.a.	2,367	0,347	0,04	n.a.	MB
6	11,04	n.a.	254,159	34,897	4,25	n.a.	BMB
Total:			1746,339	820,828	100,00	0,000	

(b)

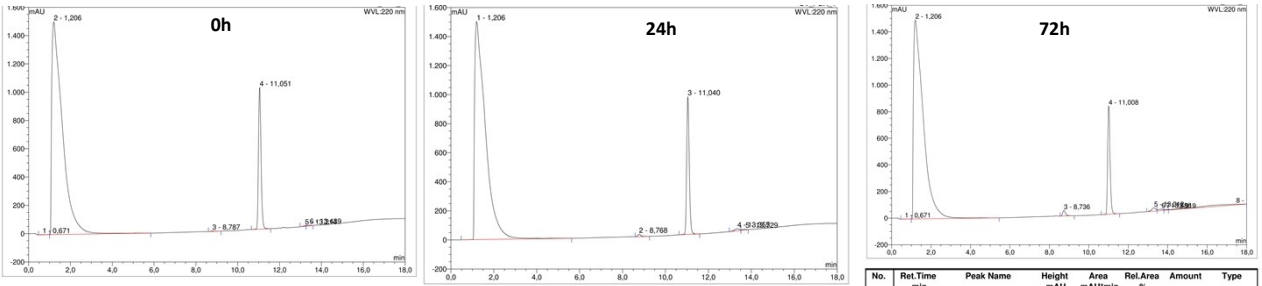

No.	Ret.Time min	Peak Name	Height mAU	Area mAU*min	Rel.Area %	Amount	Type
1	0,67	n.a.	1,236	0,363	0,04	n.a.	BMB
2	1,21	n.a.	1504,822	887,981	85,95	n.a.	BMB
3	8,79	n.a.	2,905	0,532	0,05	n.a.	BMB
4	11,05	n.a.	1001,266	142,668	13,81	n.a.	BMB
5	13,21	n.a.	3,848	0,543	0,05	n.a.	BM
6	13,44	n.a.	4,854	0,994	0,10	n.a.	MB
Total:			2518,931	1033,081	100,00	0,000	

No.	Ret.Time min	Peak Name	Height mAU	Area mAU*min	Rel.Area %	Amount	Type
1	1,21	n.a.	1500,714	871,278	86,15	n.a.	BMB
2	8,77	n.a.	15,749	2,723	0,27	n.a.	BMB
3	11,04	n.a.	948,189	132,444	13,10	n.a.	BMB
4	13,36	n.a.	13,872	3,636	0,36	n.a.	BM
5	13,73	n.a.	5,270	1,241	0,12	n.a.	MB
Total:			2483,794	1011,321	100,00	0,000	

No.	Ret.Time min	Peak Name	Height mAU	Area mAU*min	Rel.Area %	Amount	Type
1	0,67	n.a.	1,321	0,380	0,04	n.a.	BMB
2	1,21	n.a.	1494,637	855,735	84,73	n.a.	BMB
3	8,74	n.a.	41,901	7,081	0,70	n.a.	BMB
4	11,01	n.a.	813,787	113,942	11,28	n.a.	BMB
5	13,31	n.a.	25,036	6,041	0,60	n.a.	BM
6	13,69	n.a.	11,397	3,156	0,31	n.a.	M
7	13,92	n.a.	6,081	1,078	0,11	n.a.	M
8	17,47	n.a.	6,229	22,563	2,23	n.a.	MB
Total:			2400,389	1009,975	100,00	0,000	

(c)

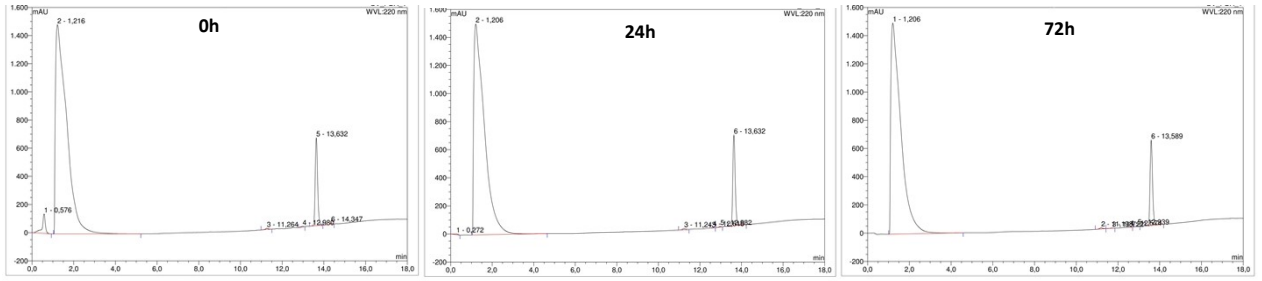

No.	Ret.Time min	Peak Name	Height mAU	Area mAU*min	Rel.Area %	Amount	Type
1	0,58	n.a.	138,222	23,569	2,28	n.a.	BMB
2	1,22	n.a.	1486,494	924,828	89,37	n.a.	BMB
3	11,26	n.a.	8,626	1,398	0,14	n.a.	BMB
4	12,98	n.a.	4,604	0,729	0,07	n.a.	BMB
5	13,63	n.a.	624,532	83,264	8,05	n.a.	BM
6	14,35	n.a.	9,589	1,098	0,11	n.a.	MB
Total:			2272,067	1034,886	100,00	0,000	

No.	Ret.Time min	Peak Name	Height mAU	Area mAU*min	Rel.Area %	Amount	Type
1	0,27	n.a.	5,382	1,344	0,14	n.a.	BMB
2	1,21	n.a.	1502,761	883,998	90,77	n.a.	BMB
3	11,24	n.a.	8,671	1,496	0,15	n.a.	BMB
4	12,62	n.a.	2,487	0,303	0,03	n.a.	BMB
5	12,98	n.a.	4,093	0,539	0,06	n.a.	BMB
6	13,63	n.a.	647,574	86,181	8,85	n.a.	BMB
Total:			2170,968	973,862	100,00	0,000	

No.	Ret.Time min	Peak Name	Height mAU	Area mAU*min	Rel.Area %	Amount	Type
1	1,21	n.a.	1496,454	836,528	90,80	n.a.	BMB
2	11,20	n.a.	8,341	1,575	0,17	n.a.	BM
3	11,72	n.a.	1,572	0,454	0,05	n.a.	MB
4	12,57	n.a.	1,743	0,212	0,02	n.a.	BMB
5	12,94	n.a.	3,766	0,491	0,05	n.a.	BMB
6	13,59	n.a.	605,064	82,019	8,90	n.a.	BMB
Total:			2116,940	921,279	100,00	0,000	

Figure S 2. HPLC Chromatograms of complex 2 (a), 6 (b) and 10 (c) in DMSO-PBS (4:1; v:v) at 37 °C with different incubation times. Gradient: 30-95 % of acetonitrile in water (with 0.1 % formic acid).

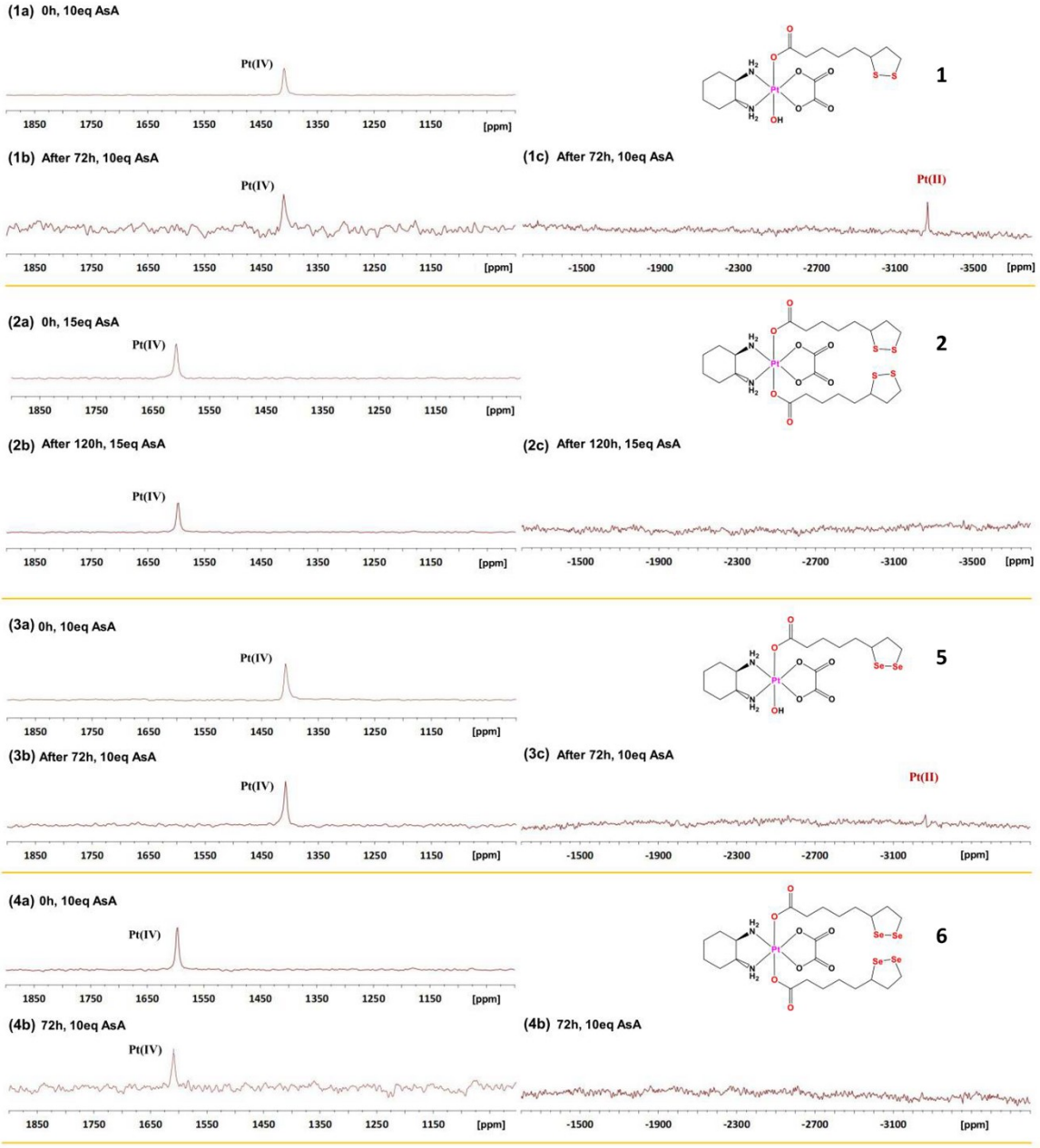

[figure continued]

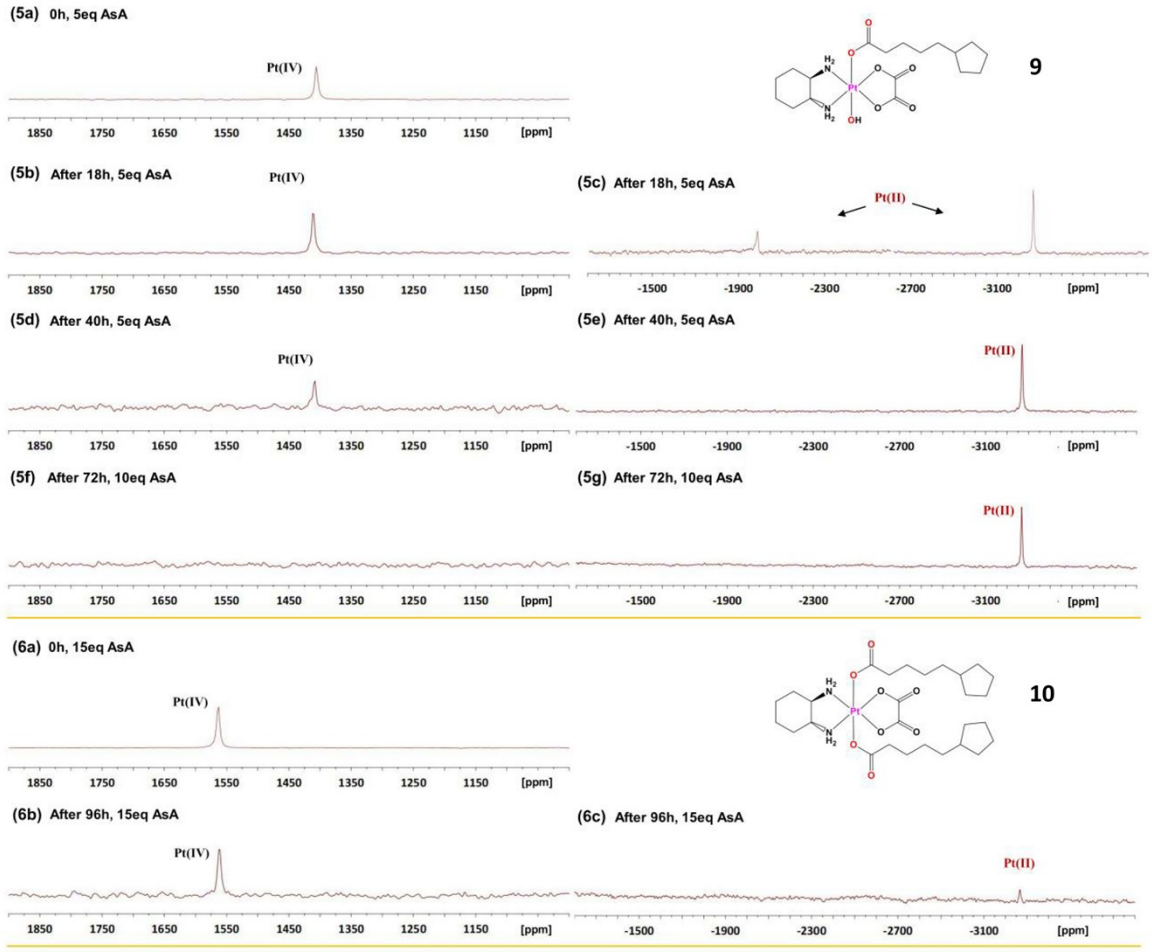

Figure S 3. ^{195}Pt NMR spectra[a] of complexes 1, 2, 5, 6, 9 and 10 (substance concentration, 8 mM) after incubation with ascorbic acid in a mixture of DMSO/PBS (V/V, 4/1, pH=7.2[b]) at 37 °C.

[a] The spectra were recorded within two ranges (500 to 2500 ppm, typically for Pt^{IV} complexes) and (-1000 to -4000 ppm, typically for Pt^{II} complexes.

[b] After addition of 10 eq of ascorbic acid, the pH of reaction solution was shifted from 7.4 to 7.2.

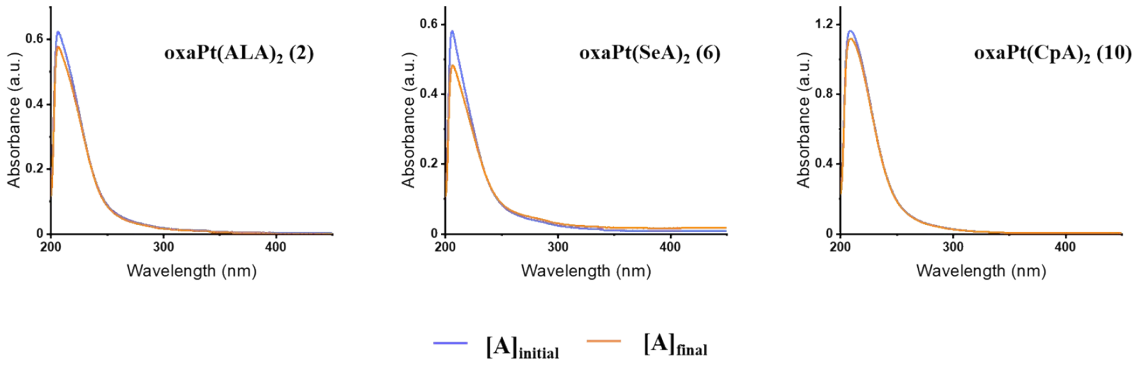

Figure S 4. UV-Vis absorption spectrum of complexes 2, 6 and 10 in octanol phase (pre-saturated with water) before (initial value, blue) and after (final value, red) mixing with water phase (pre-saturated with octanol).

Part 2. NMR spectra

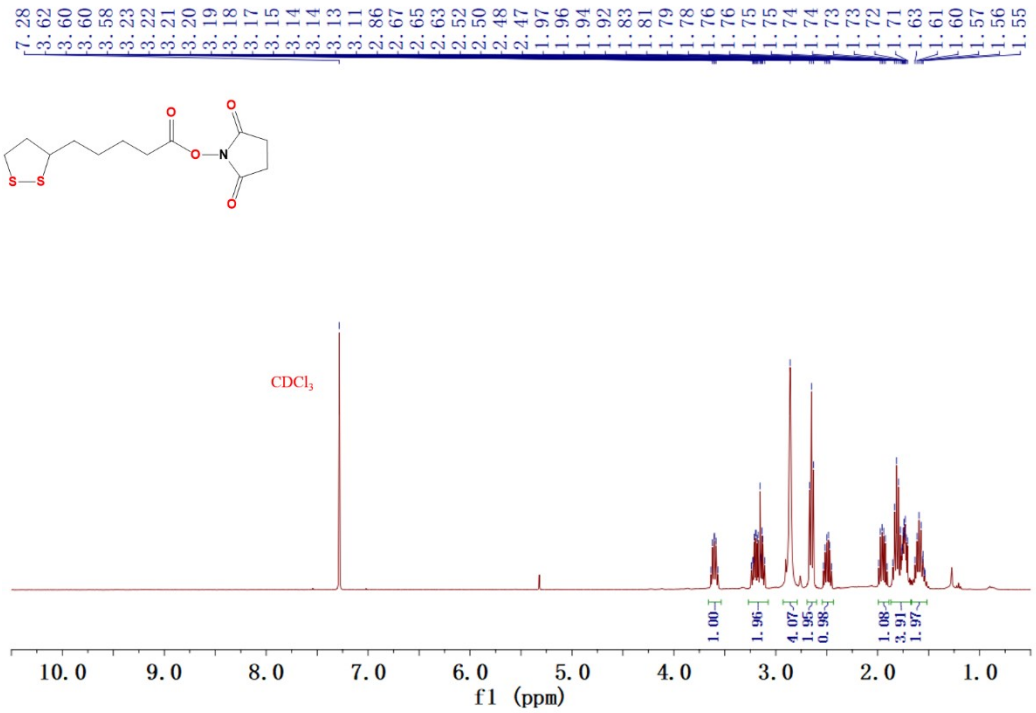

Figure S 5. ^{1}H NMR (400MHz, 297 K, $CDCl_3$) spectrum of ALA-NHS.

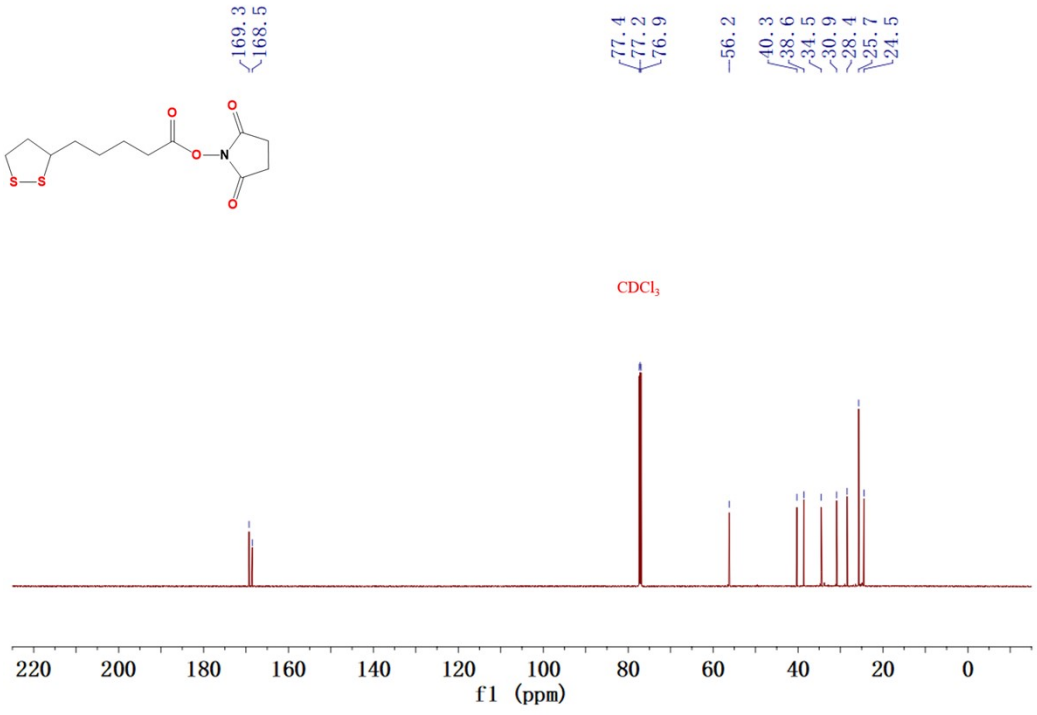

Figure S 6. $^{13}C\{^{1}H\}$ NMR (150MHz, 297 K, $CDCl_3$) spectrum of ALA-NHS.

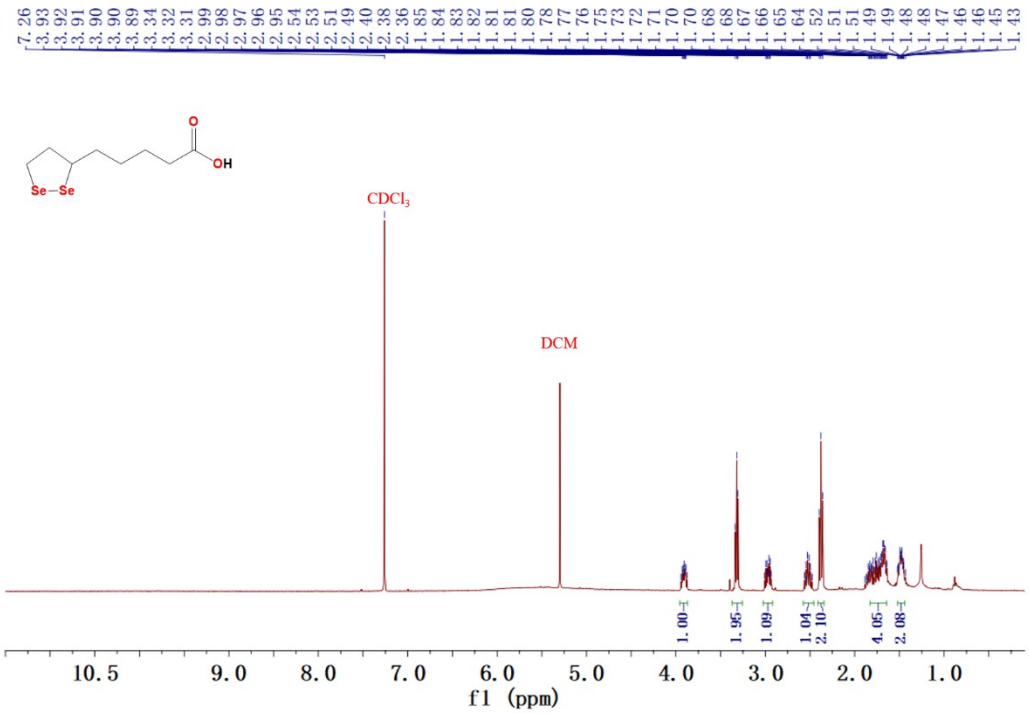

Figure S 7. ^{1}H NMR (400MHz, 297 K, $CDCl_3$) spectrum of SeA.

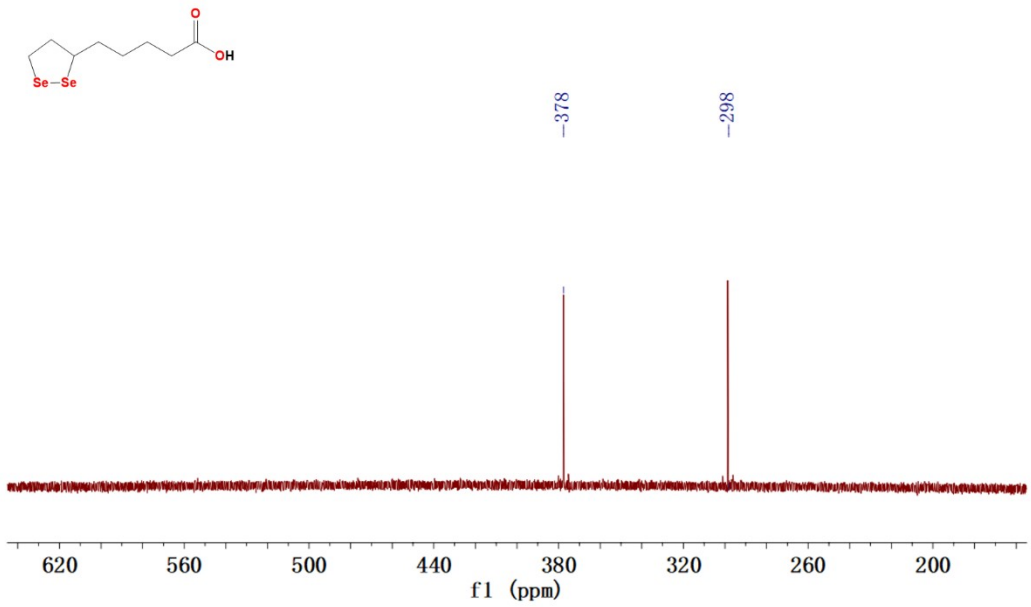

Figure S 8. ^{77}Se{^{1}H} NMR (76 MHz, 297 K, $CDCl_3$) spectrum of SeA. ($J_{Se\text{-}Se}$= 190 Hz)

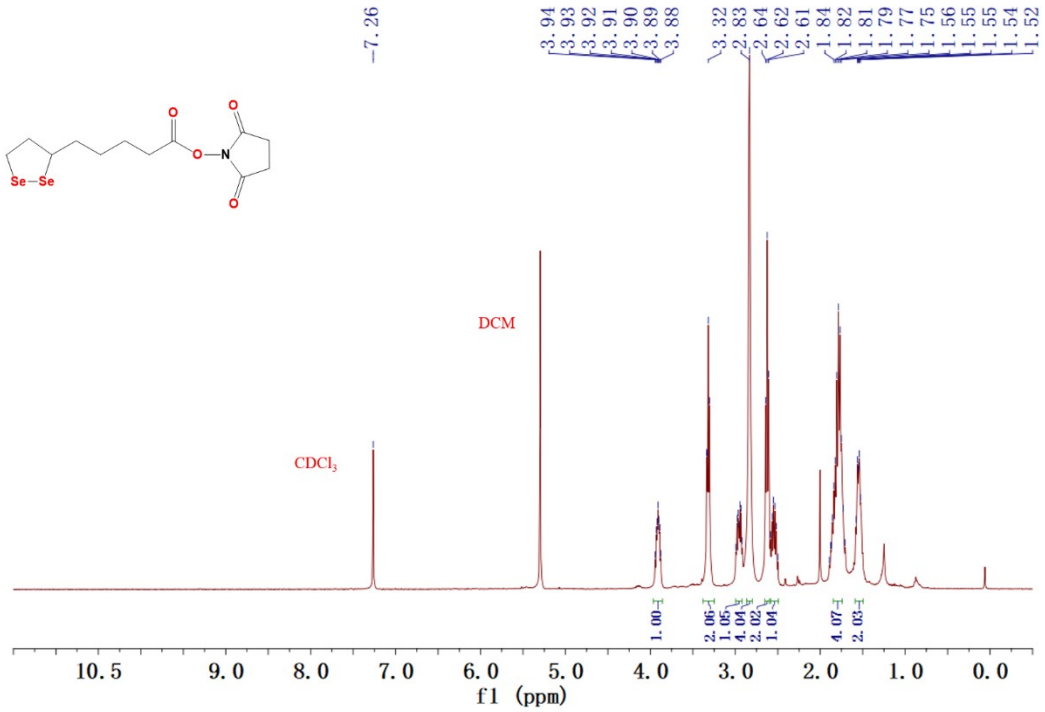

Figure S 9. ^{1}H NMR (400MHz, 297 K, $CDCl_3$) spectrum of SeA-NHS.

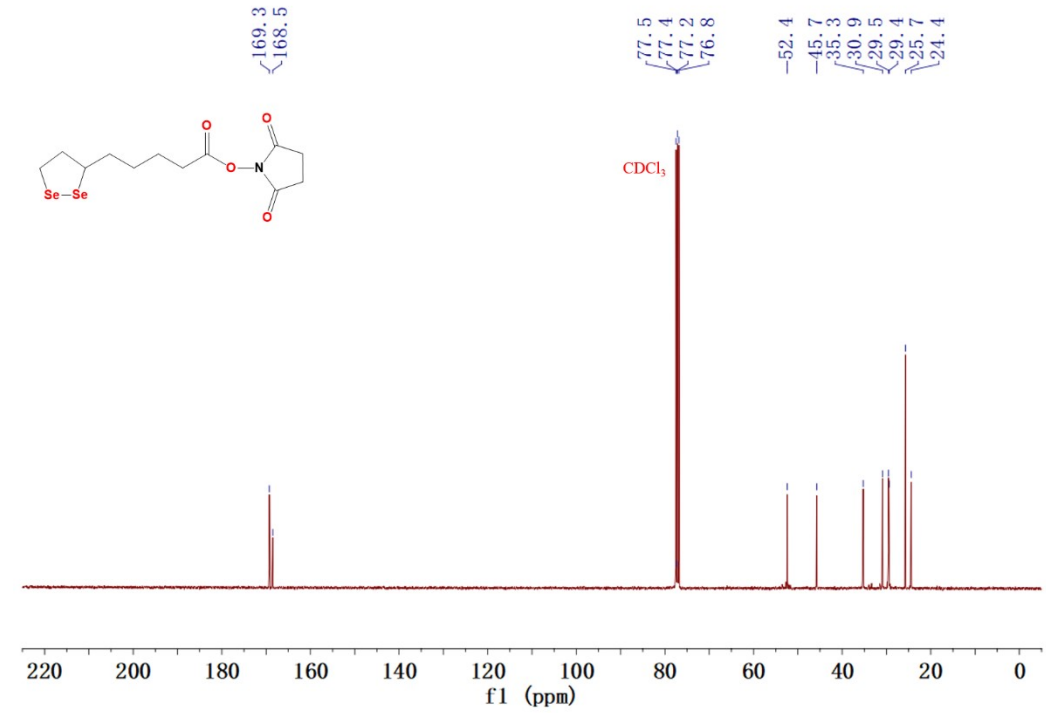

Figure S 10. $^{13}C\{^{1}H\}$ NMR (100MHz, 297 K, $CDCl_3$) spectrum of SeA-NHS.

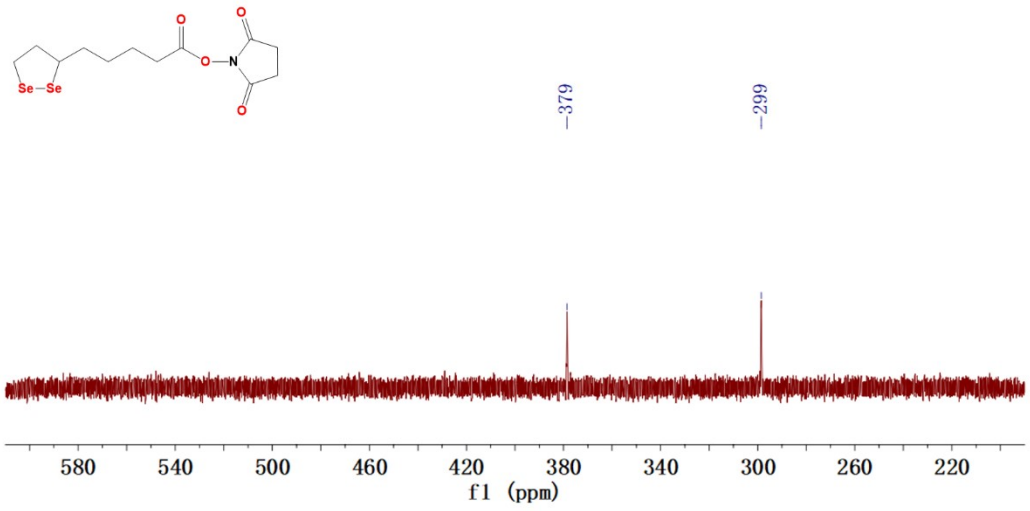

Figure S 11. $^{77}Se\{^{1}H\}$ NMR (76 MHz, 297 K, $CDCl_3$) spectrum of SeA-NHS.

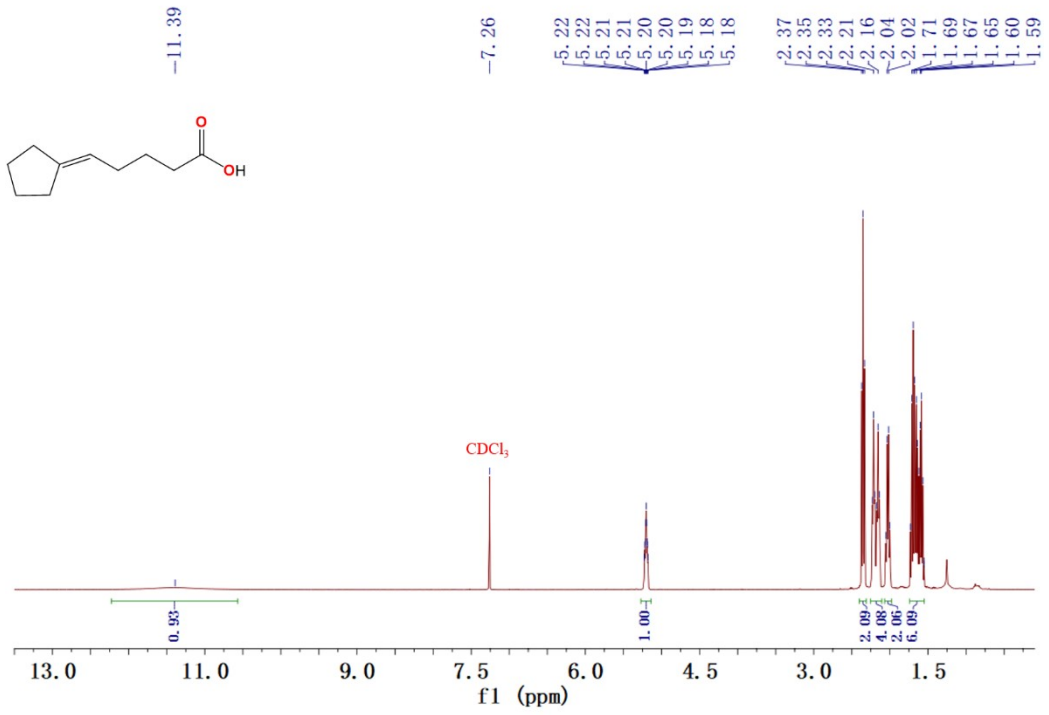

Figure S 12. ^{1}H NMR (400MHz, 297 K, $CDCl_3$) spectrum of 5-cyclopenylidene-pentanoic acid.

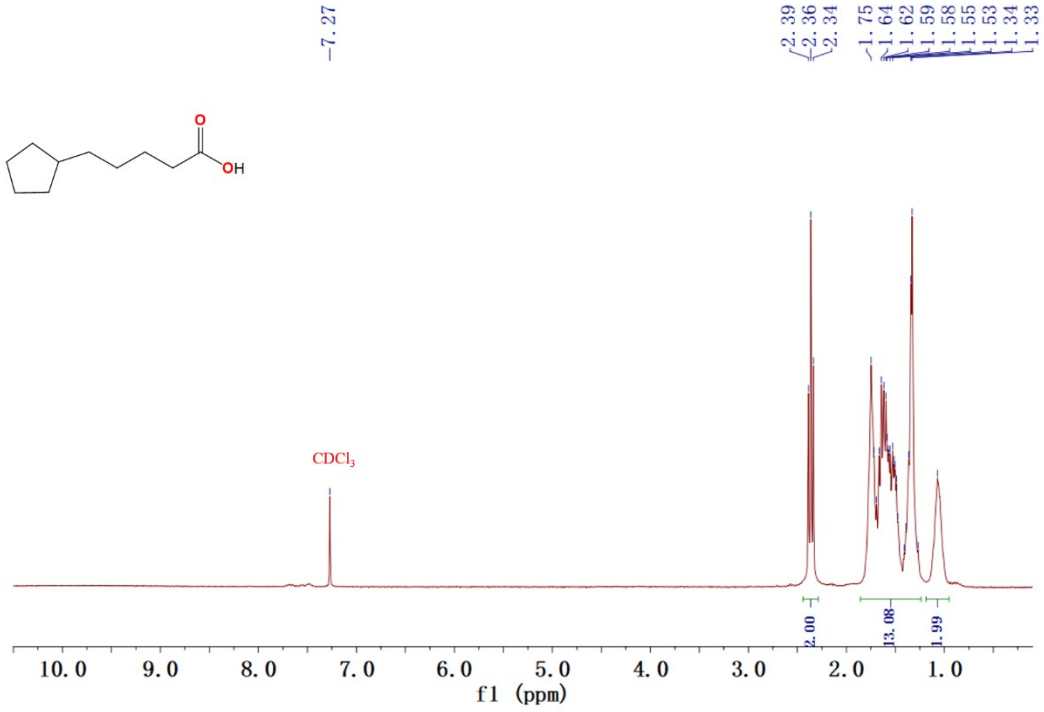

Figure S 13. ^{1}H NMR (300MHz, 297 K, $CDCl_3$) spectrum of CpA.

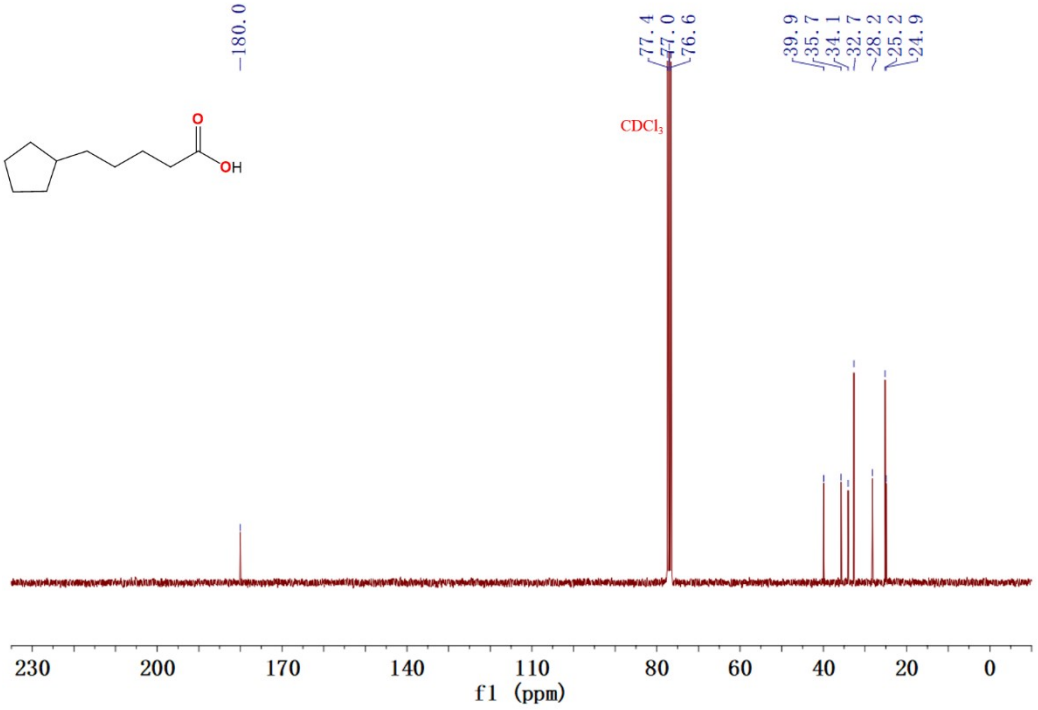

Figure S 14. $^{13}C\{^{1}H\}$ NMR (75MHz, 297 K, $CDCl_3$) spectrum of CpA.

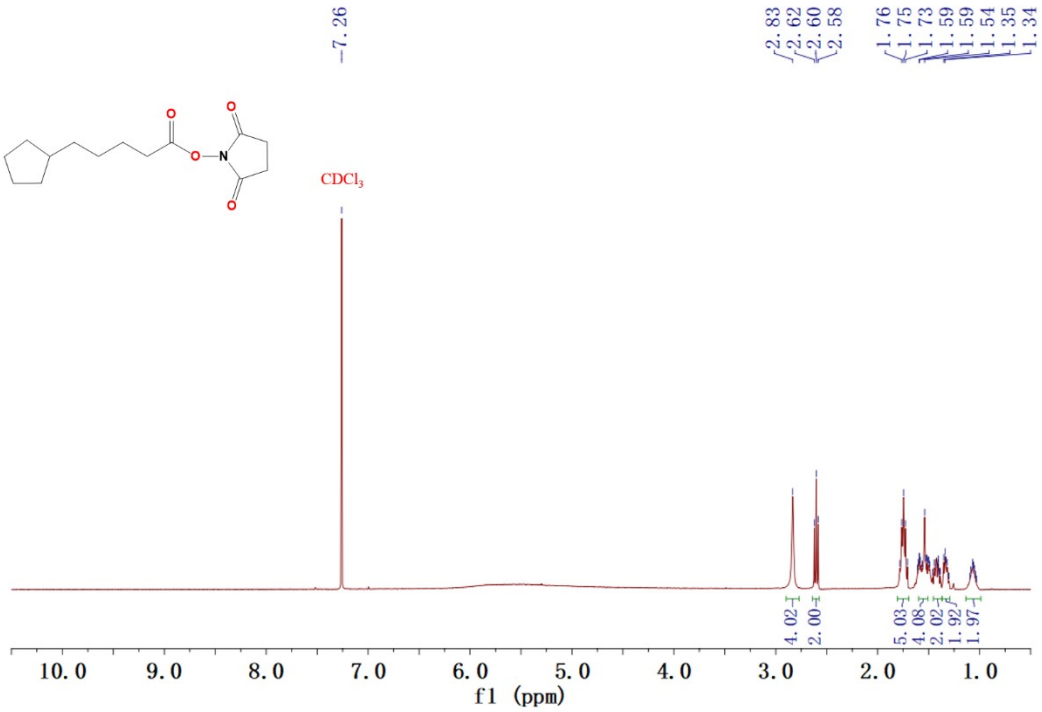

Figure S 15. ^{1}H NMR (400MHz, 297 K, $CDCl_3$) spectrum of CpA-NHS.

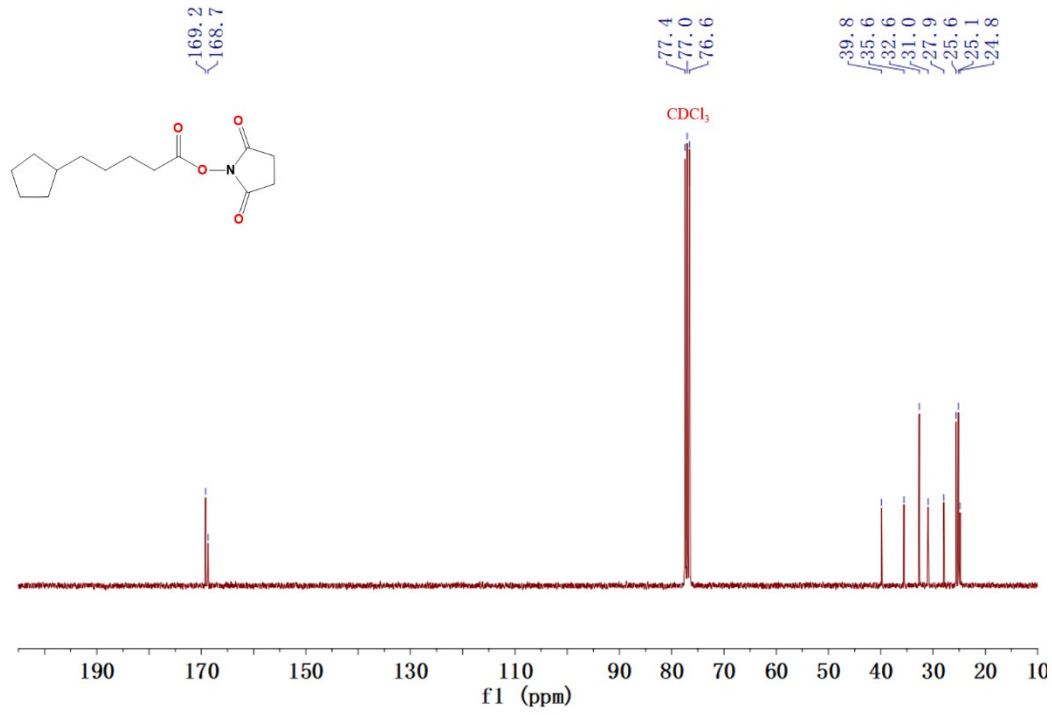

Figure S 16. $^{13}C\{^{1}H\}$ NMR (100MHz, 297 K, $CDCl_3$) spectrum of CpA-NHS.

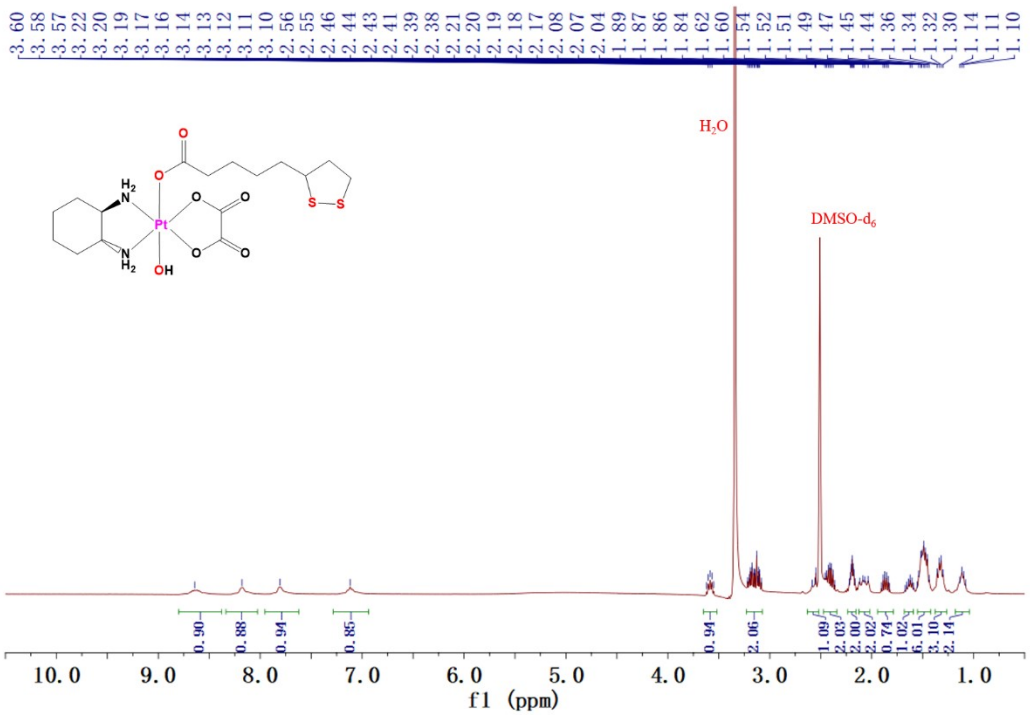

Figure S 17. ^{1}H NMR (400MHz, 297 K, DMSO-d$_6$) spectrum of complex 1.

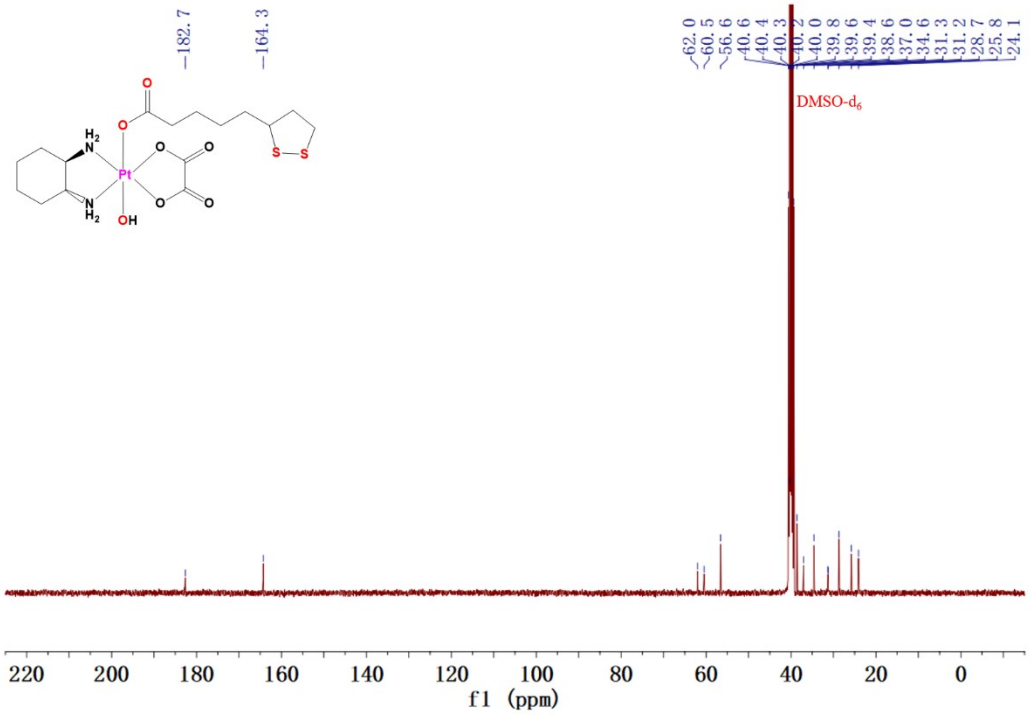

Figure S 18. ^{13}C{^{1}H} NMR (100MHz, 297 K, DMSO-d$_6$) spectrum of complex 1.

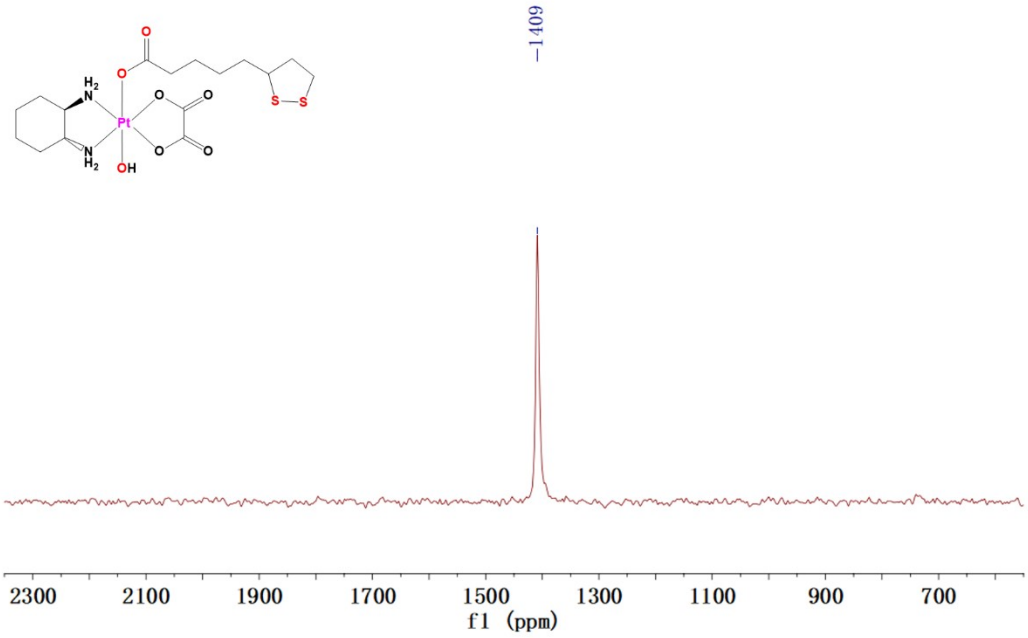

Figure S 19. $^{195}Pt\{^{1}H\}$ NMR (86MHz, 297 K, DMSO-d_6) spectrum of complex 1.

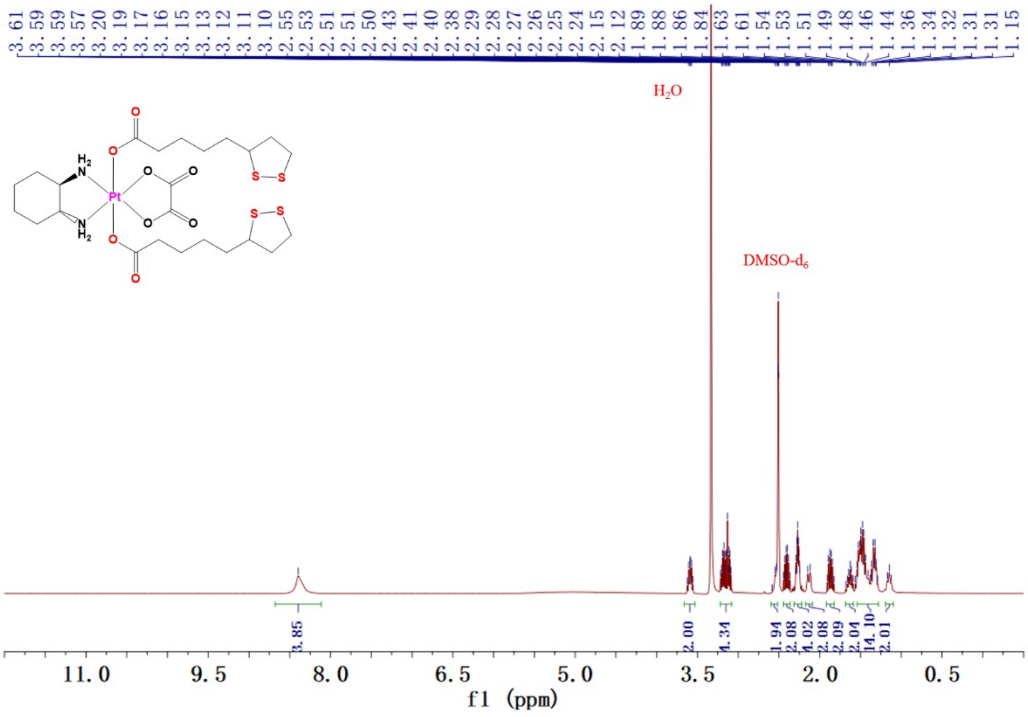

Figure S 20. ^{1}H NMR (400MHz, 297 K, DMSO-d_6) spectrum of complex 2.

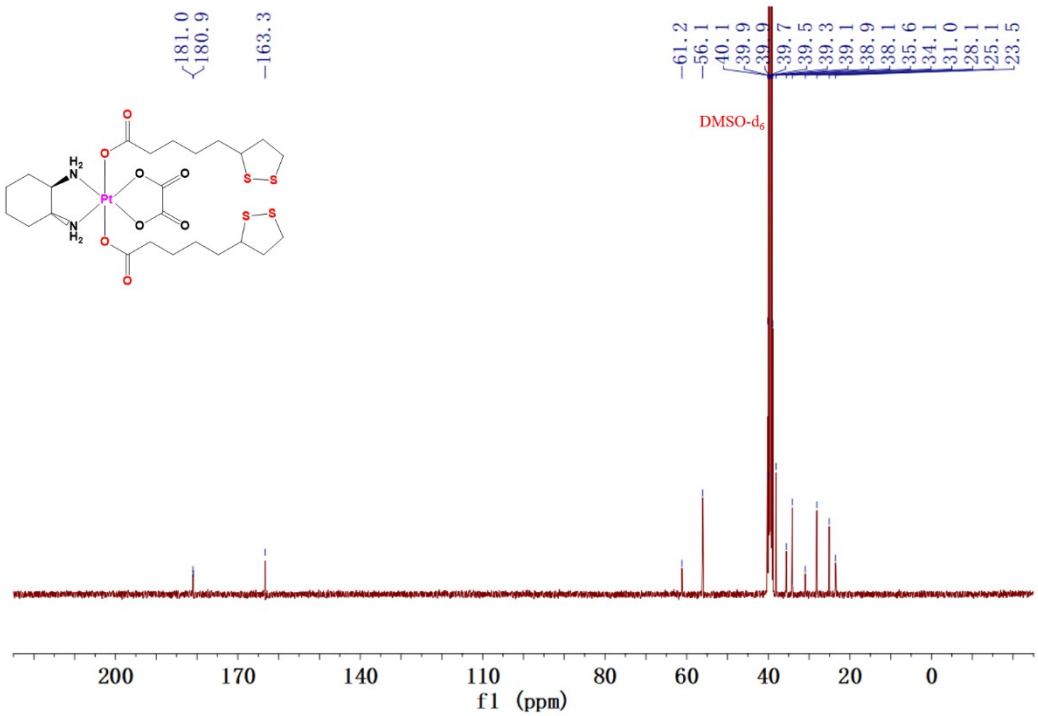

Figure S 21. $^{13}C\{^{1}H\}$ NMR (100MHz, 297 K, DMSO-d_6) spectrum of complex 2.

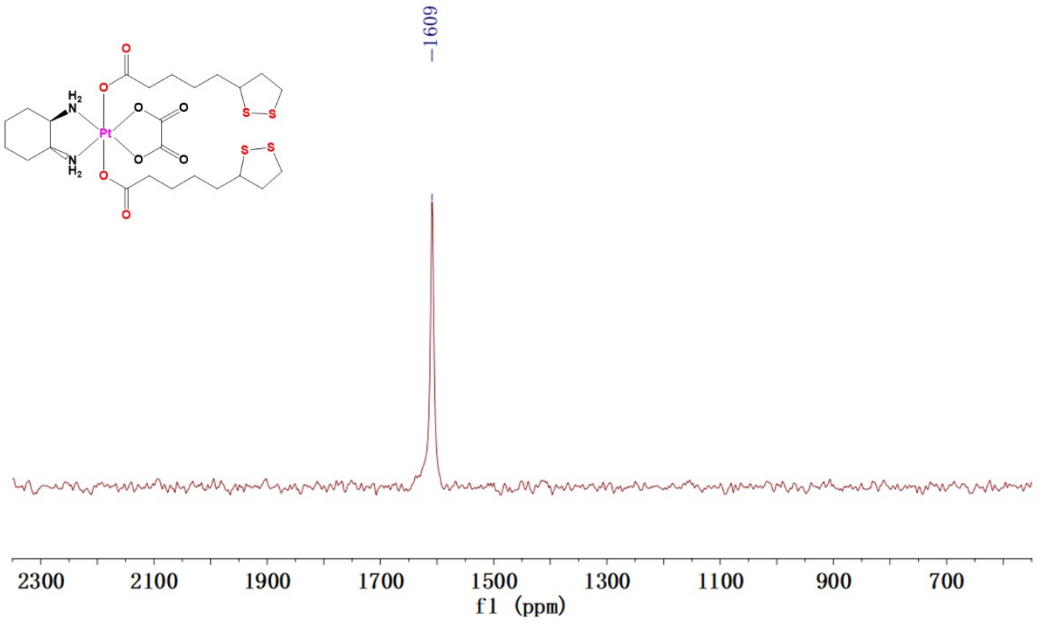

Figure S 22. $^{195}Pt\{^{1}H\}$ NMR (86MHz, 297 K, DMSO-d_6) spectrum of complex 2.

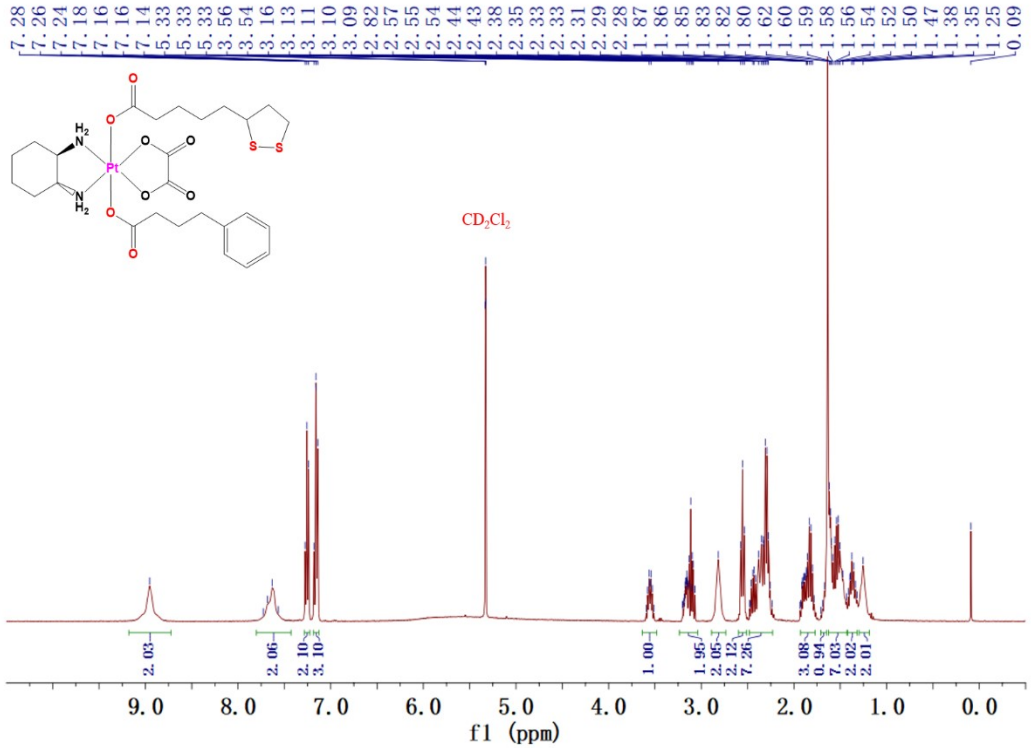

Figure S 23. ^{1}H NMR (400MHz, 297 K, CD_2Cl_2) spectrum of complex 3.

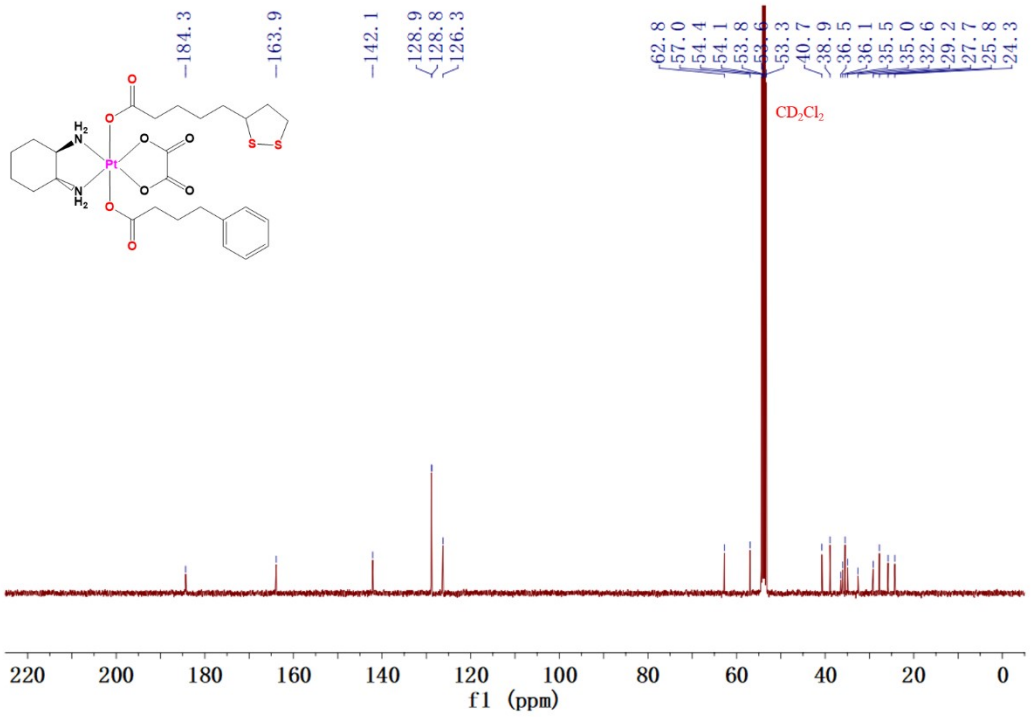

Figure S 24. $^{13}C\{^{1}H\}$ NMR (100MHz, 297 K, CD_2Cl_2) spectrum of complex 3.

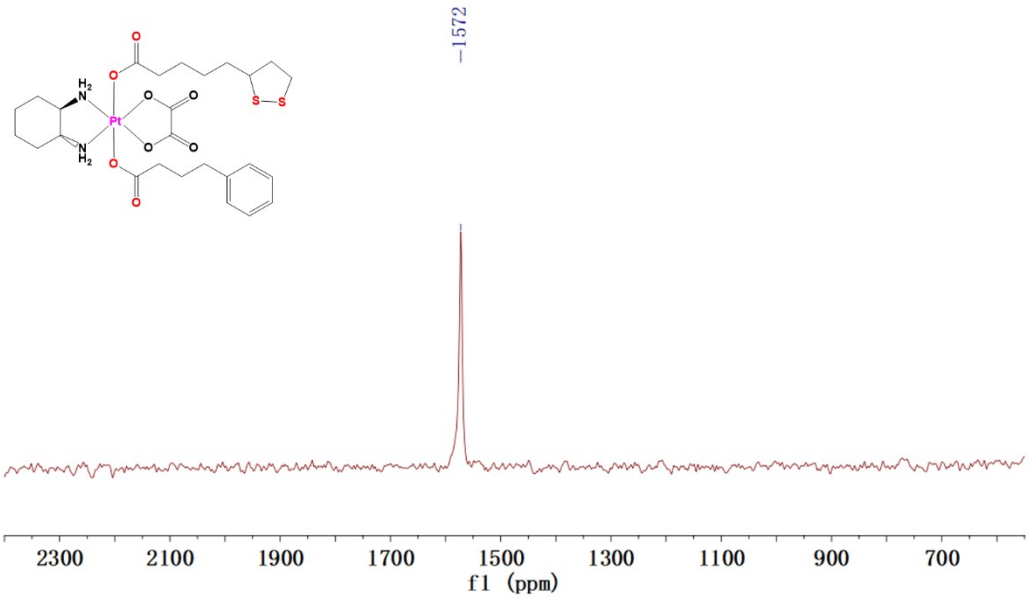

Figure S 25. $^{195}Pt\{^{1}H\}$ NMR (86MHz, 297 K, CD_2Cl_2) spectrum of complex 3.

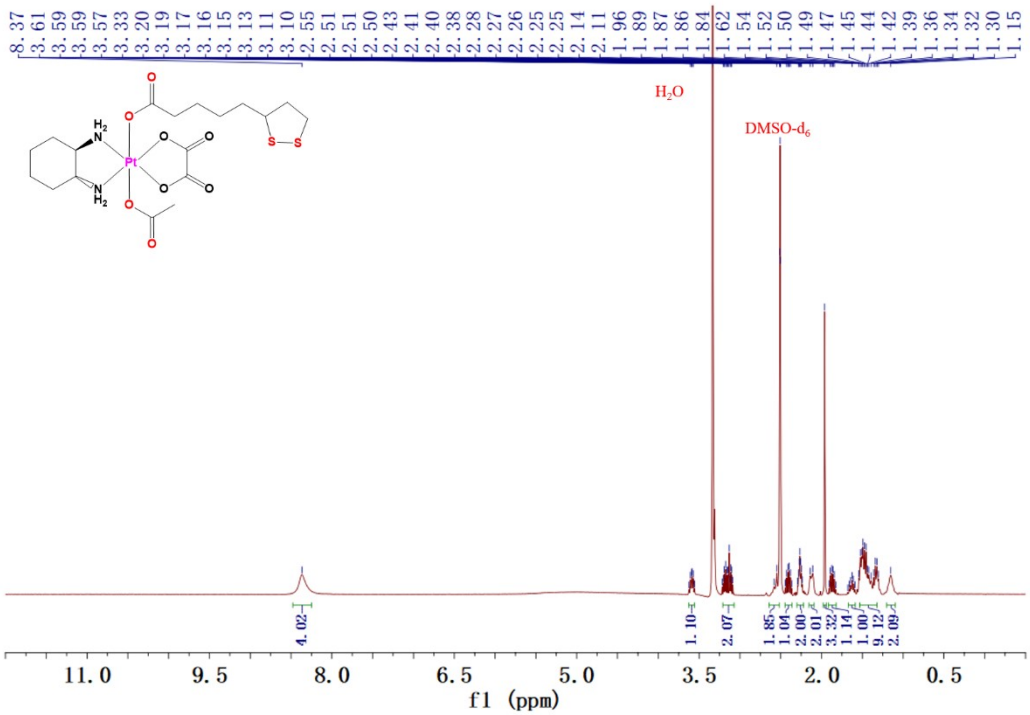

Figure S 26. ^{1}H NMR (400MHz, 297 K, DMSO-d_6) spectrum of complex 4.

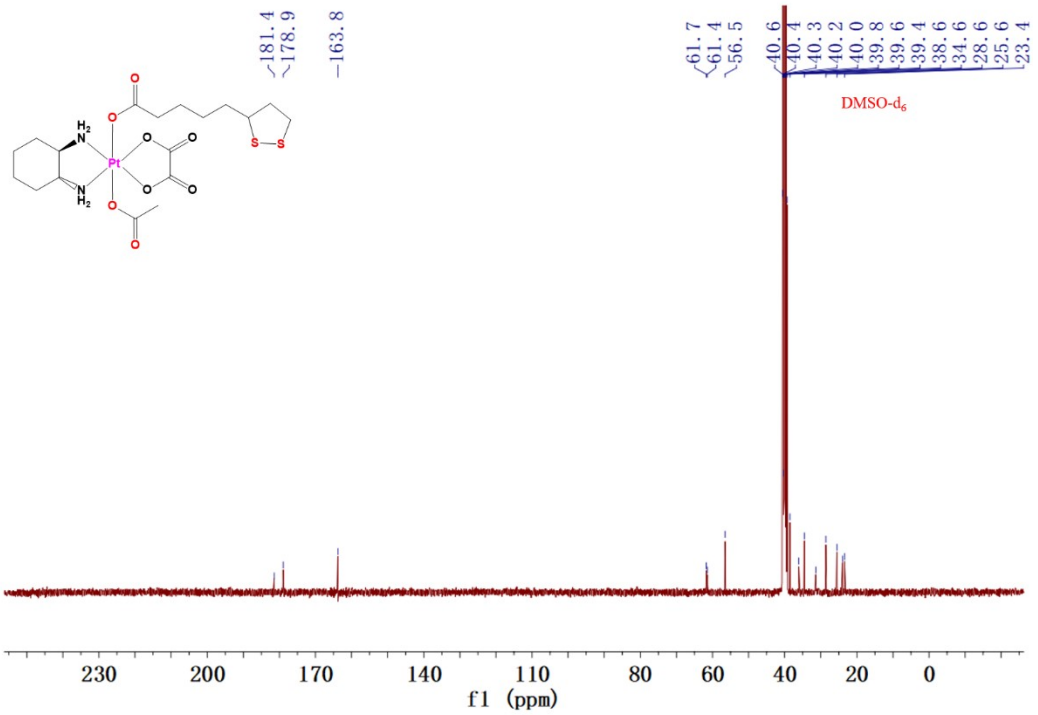

Figure S 27. $^{13}C\{^1H\}$ NMR (100MHz, 297 K, DMSO-d_6) spectrum of complex 4.

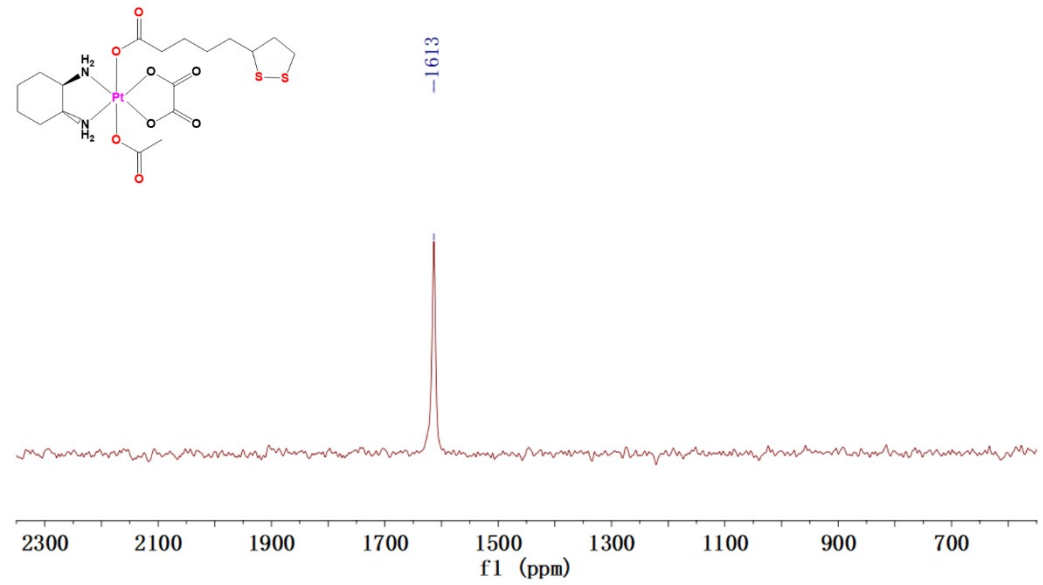

Figure S 28. $^{195}Pt\{^1H\}$ NMR (86MHz, 297 K, DMSO-d_6) spectrum of complex 4.

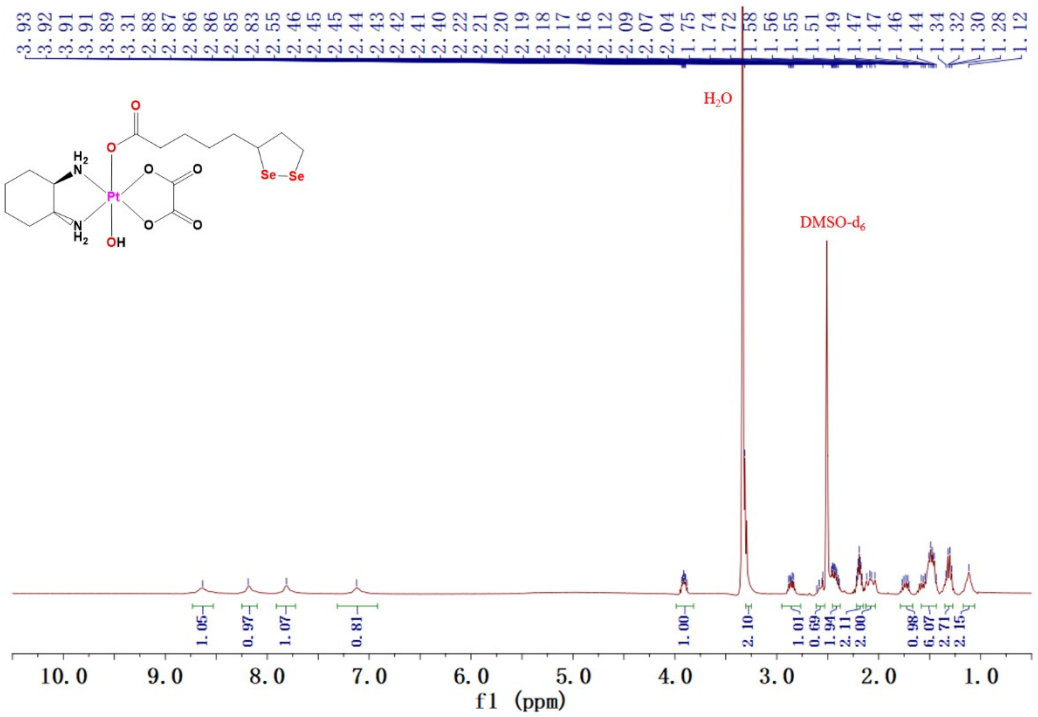

Figure S 29. ^{1}H NMR (400MHz, 297 K, DMSO-d$_6$) spectrum of complex 5.

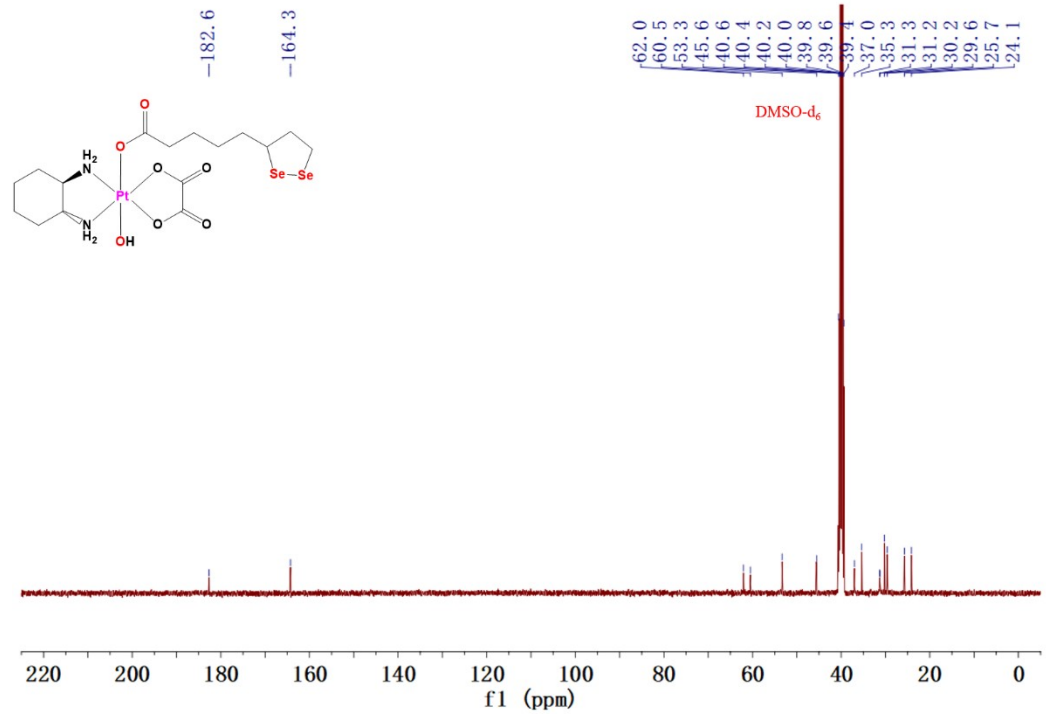

Figure S 30. ^{13}C{^{1}H} NMR (100MHz, 297 K, DMSO-d$_6$) spectrum of complex 5.

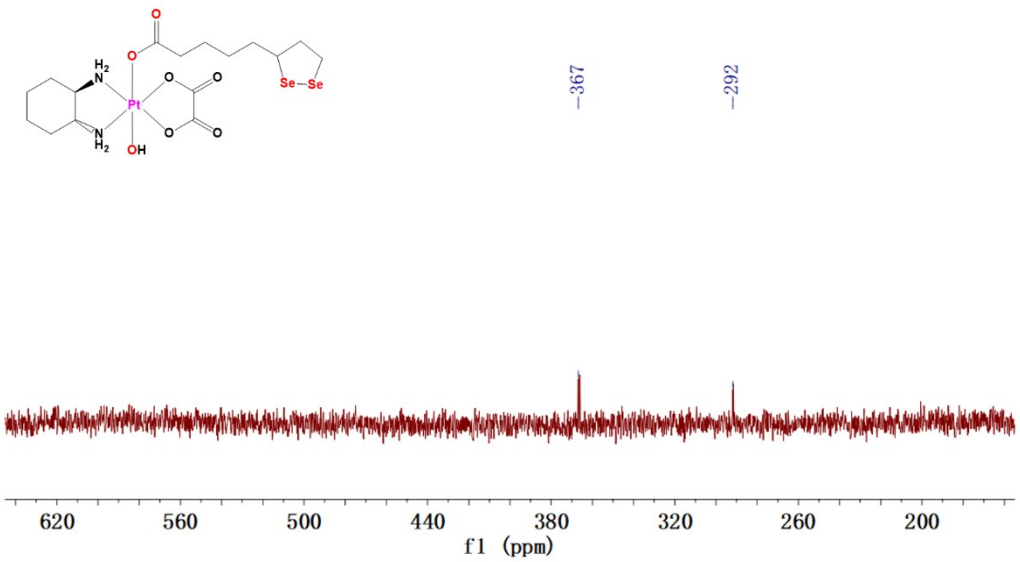

Figure S 31. $^{77}Se\{^{1}H\}$ NMR (76MHz, 297 K, DMSO-d_6) spectrum of complex 5.

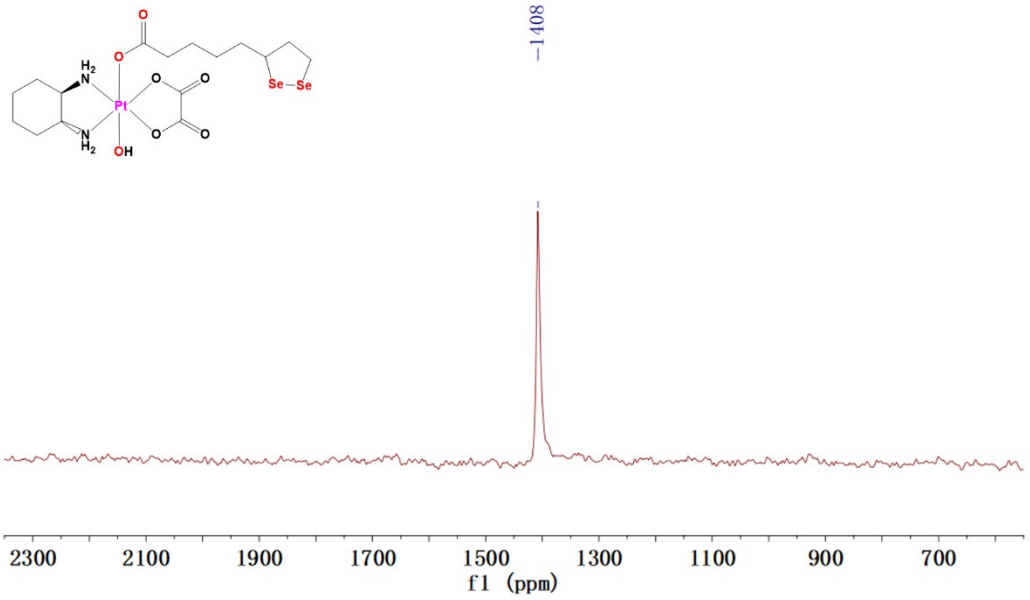

Figure S 32. $^{195}Pt\{^{1}H\}$ NMR (86MHz, 297 K, DMSO-d_6) spectrum of complex 5.

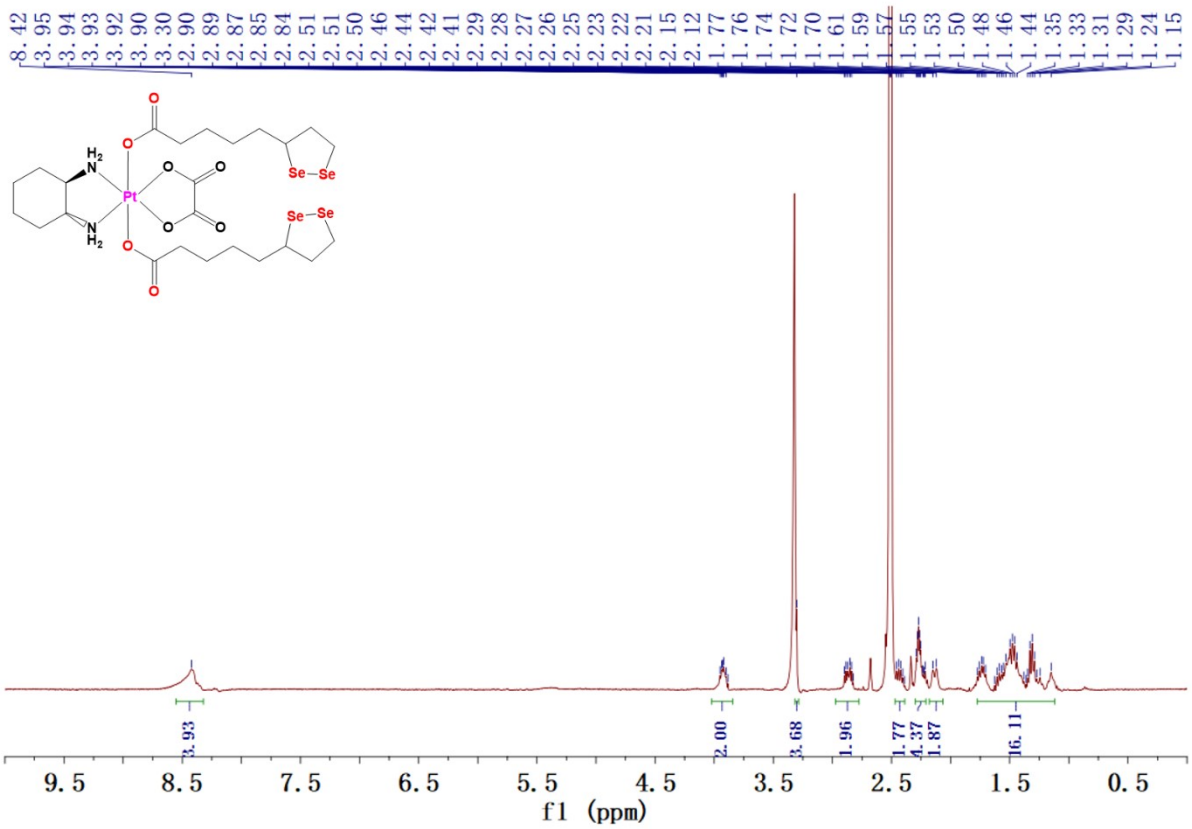

Figure S 33. ^{1}H NMR (400MHz, 297 K, DMSO-d_6) spectrum of complex 6.

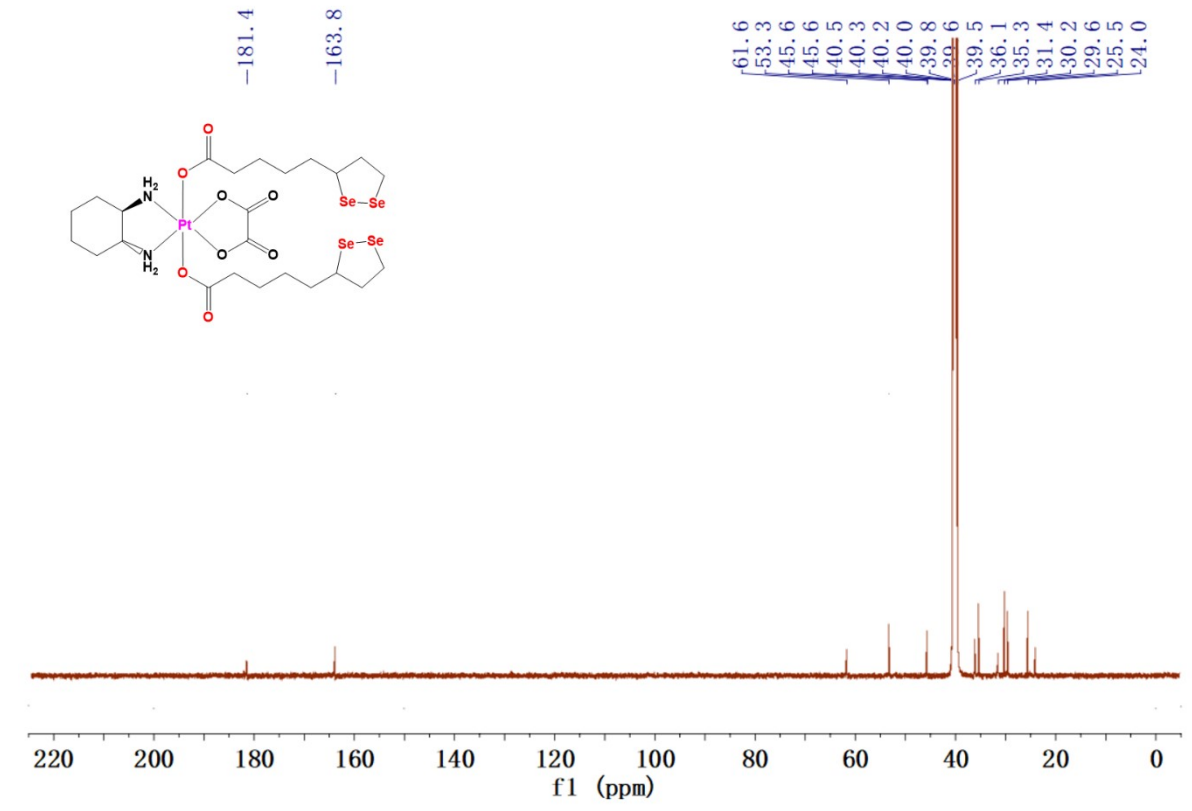

Figure S 34. ^{13}C NMR{^{1}H} (125MHz, 297 K, DMSO-d_6) spectrum of complex 6.

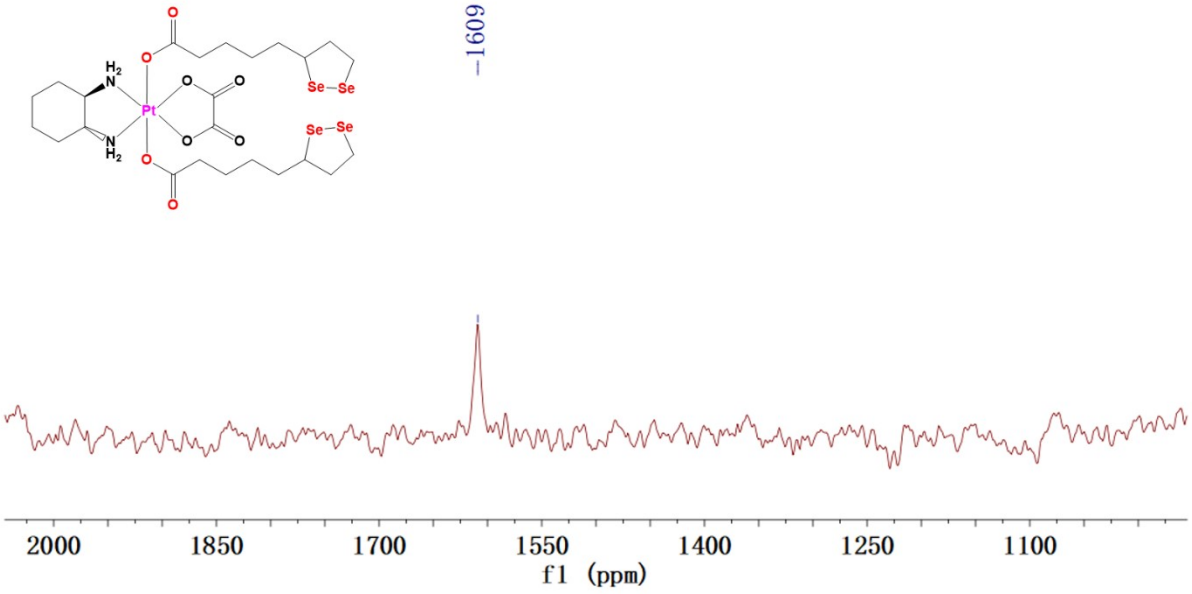

Figure S 35. $^{195}Pt\{^{1}H\}$ NMR (86MHz, 297 K, DMSO-d_6) spectrum of complex 6.

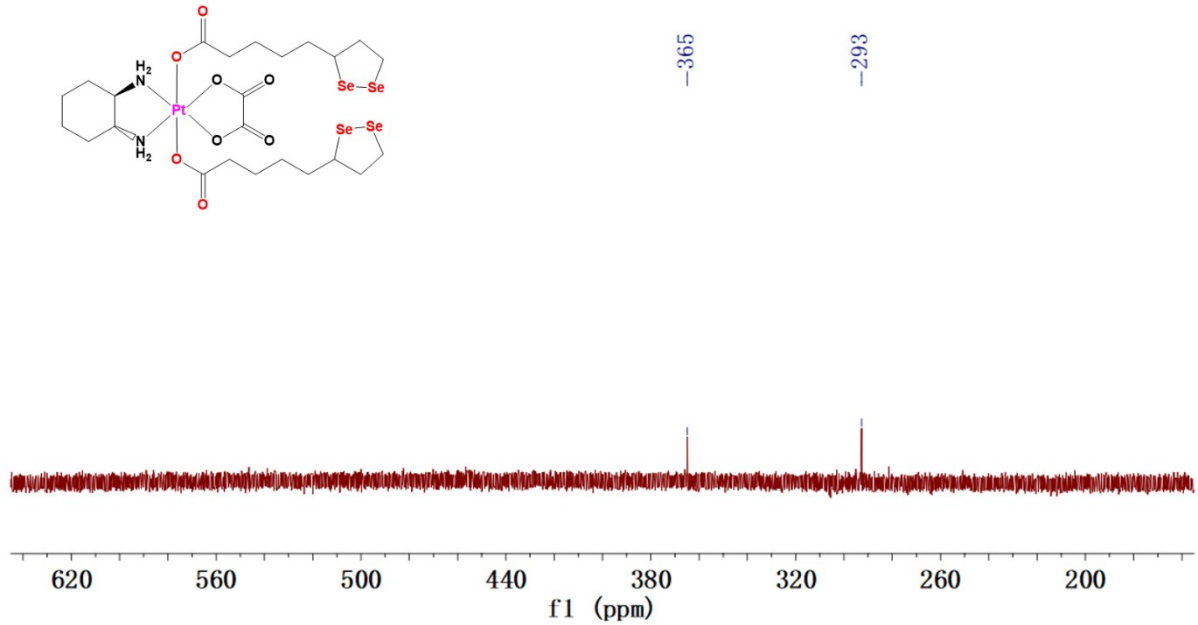

Figure S 36. $^{77}Se\{^{1}H\}$ NMR (76MHz, 297 K, DMSO-d_6) spectrum of complex 6.

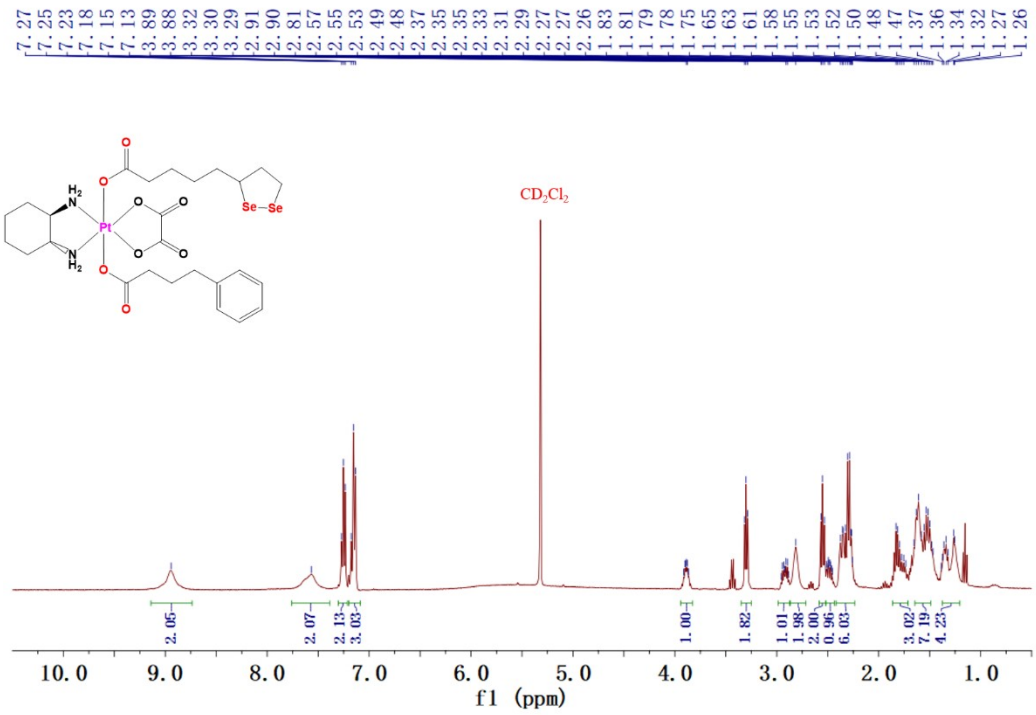

Figure S 37. ^{1}H NMR (400MHz, 297 K, CD_2Cl_2) spectrum of complex 7.

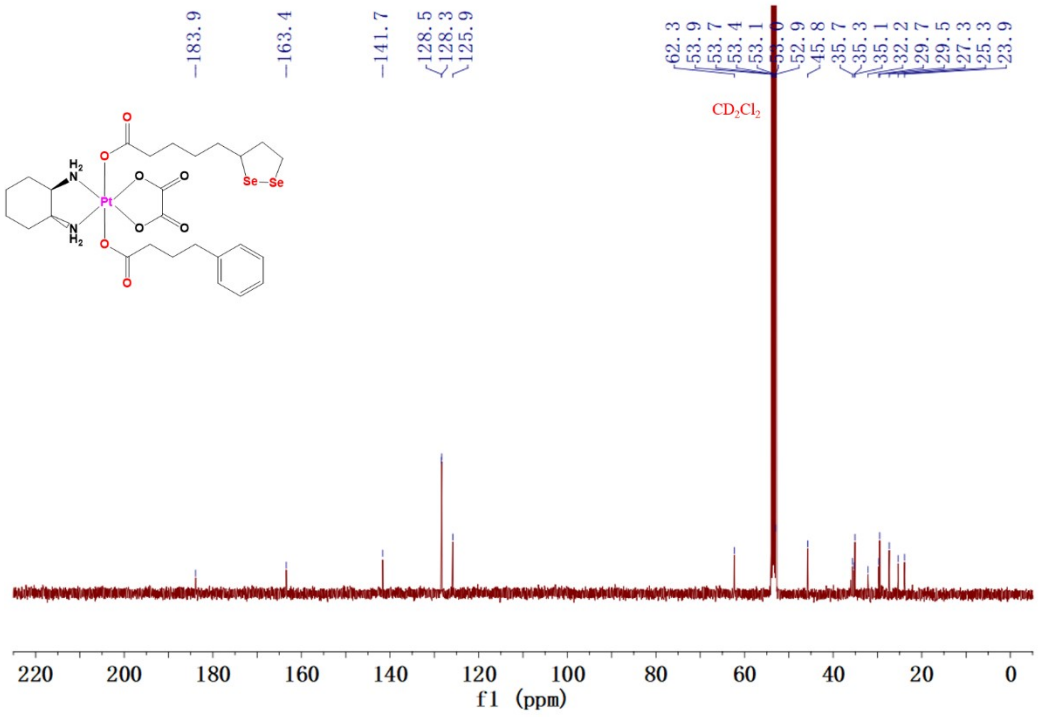

Figure S 38. $^{13}C\{^{1}H\}$ NMR (100MHz, 297 K, CD_2Cl_2) spectrum of complex 7.

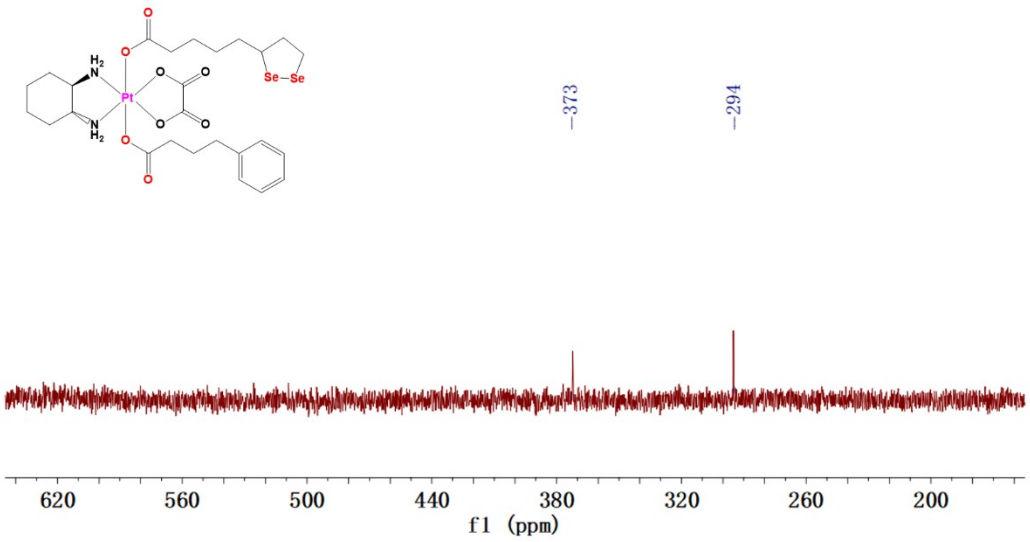

Figure S 39. $^{77}Se\{^{1}H\}$ NMR (76MHz, 297 K, CD_2Cl_2) spectrum of complex 7.

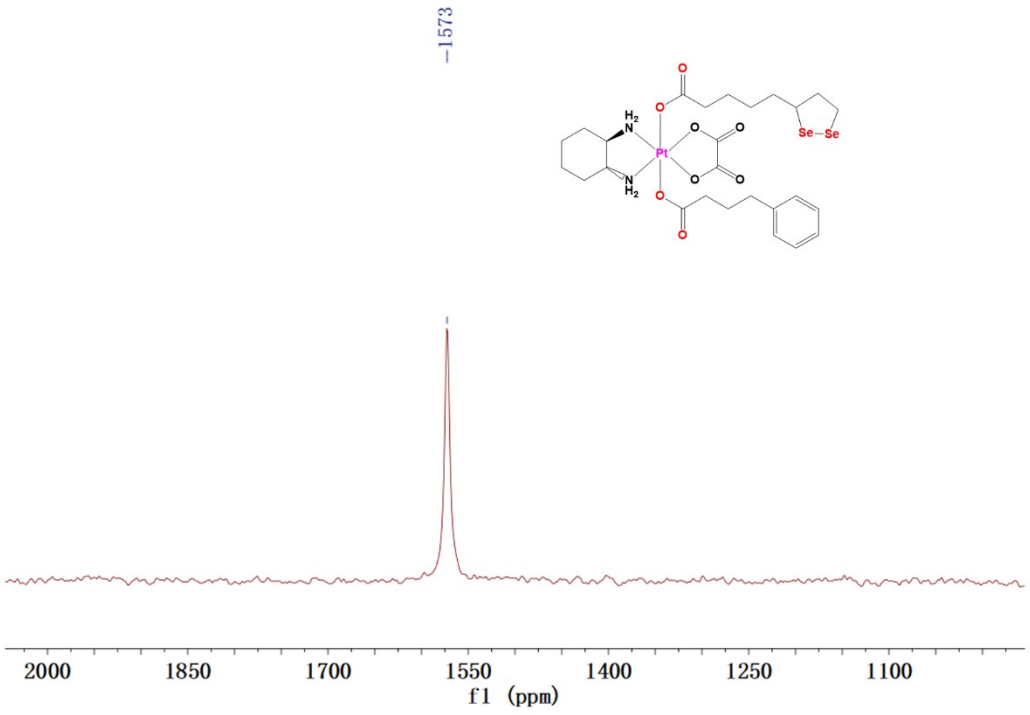

Figure S 40. $^{195}Pt\{^{1}H\}$ NMR (86MHz, 297 K, CD_2Cl_2) spectrum of complex 7.

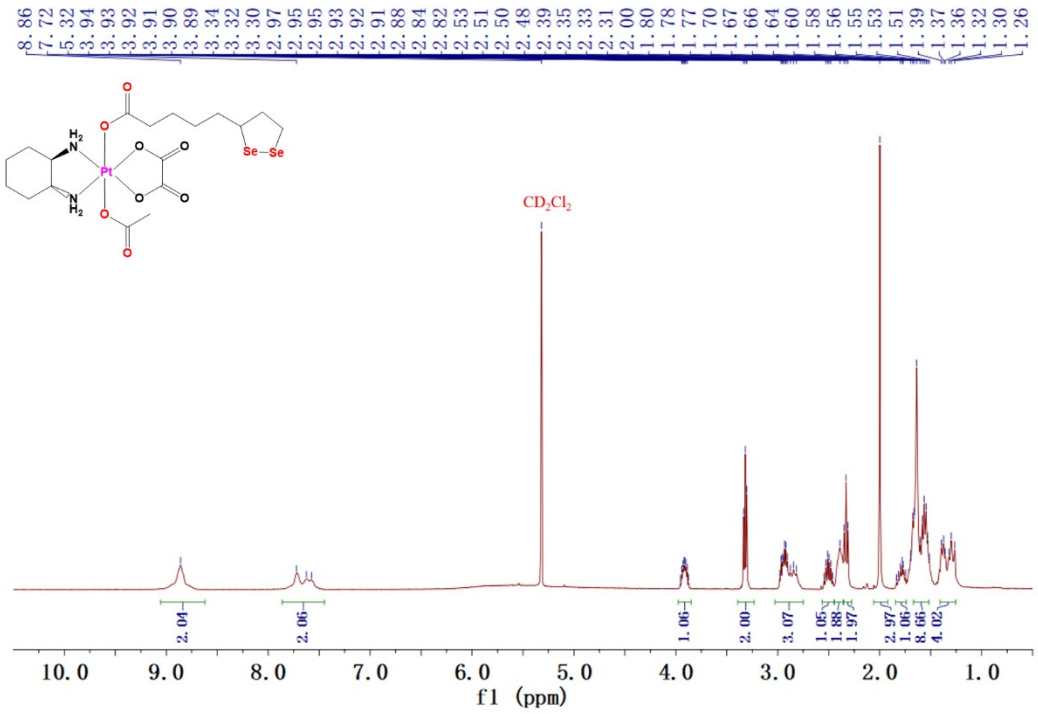

Figure S 41. ^{1}H NMR (400MHz, 297 K, CD_2Cl_2) spectrum of complex 8.

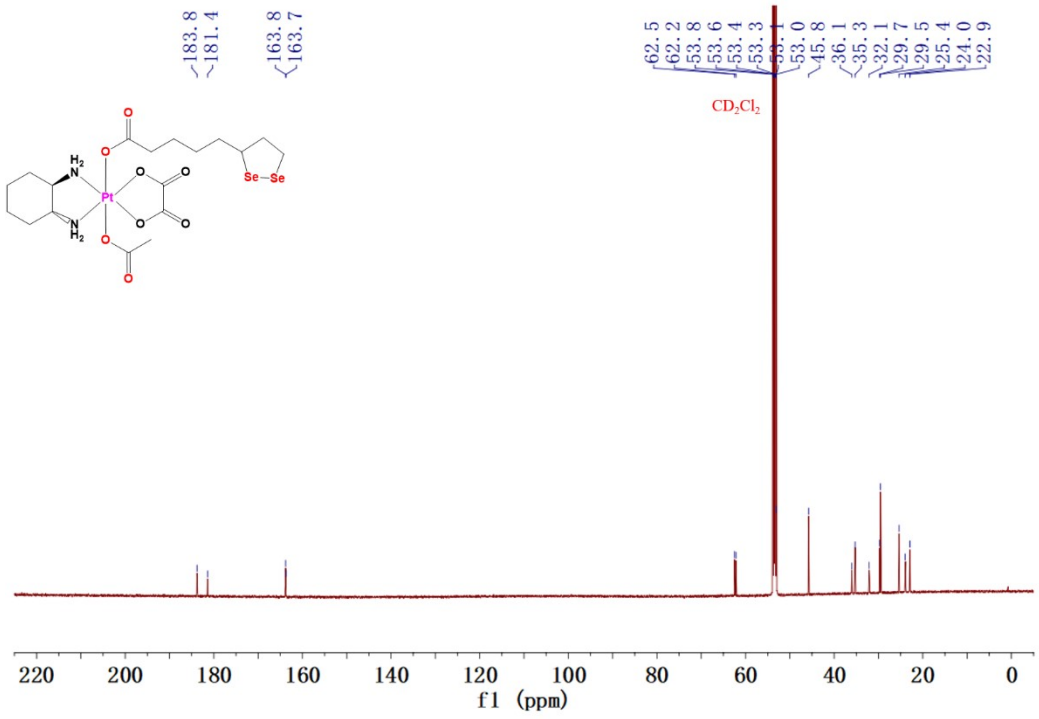

Figure S 42. $^{13}C\{^{1}H\}$ NMR (100MHz, 297 K, CD_2Cl_2) spectrum of complex 8.

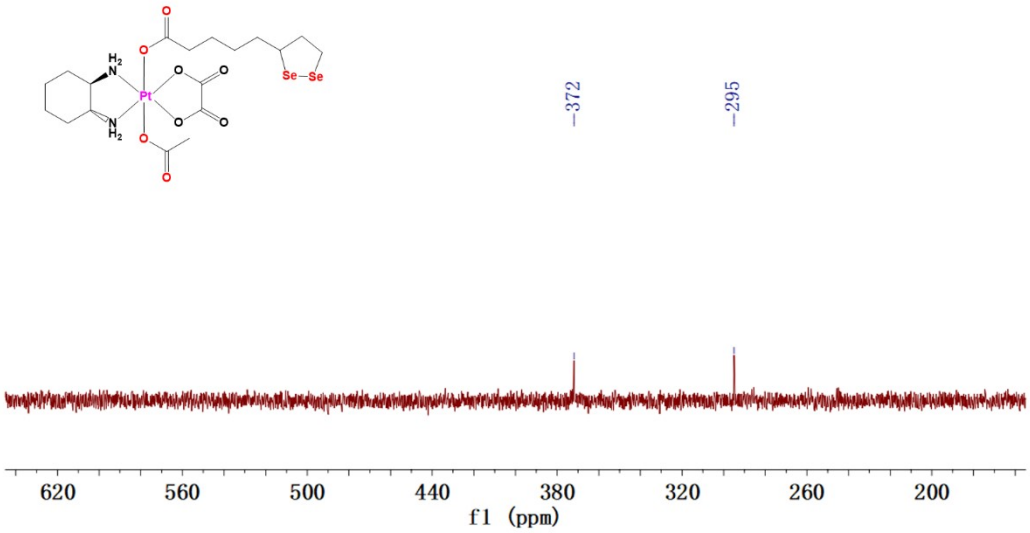

Figure S 43. $^{77}Se\{^{1}H\}$ NMR (76MHz, 297 K, CD_2Cl_2) spectrum of complex 8.

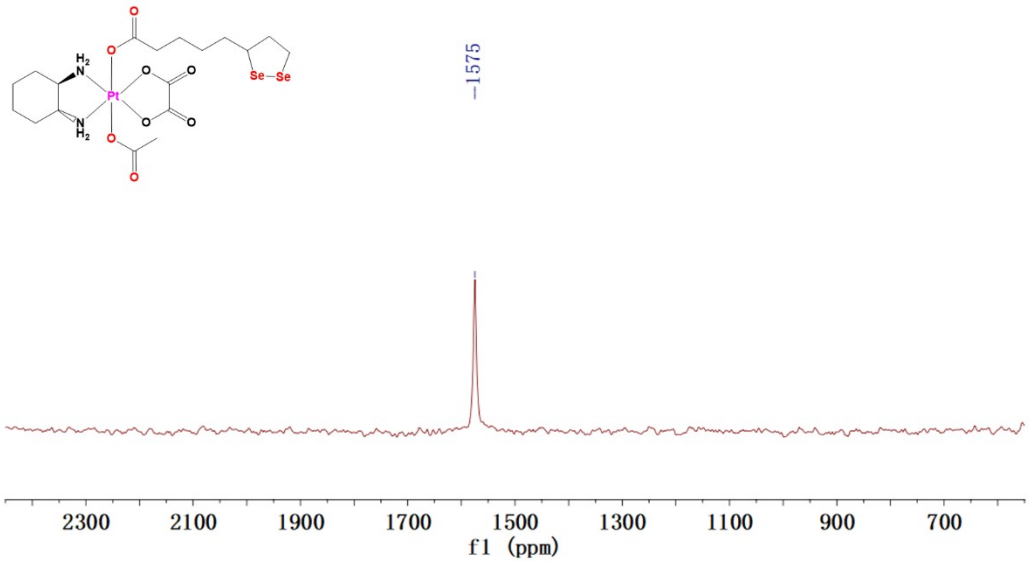

Figure S 44. $^{195}Pt\{^{1}H\}$ NMR (86MHz, 297 K, CD_2Cl_2) spectrum of complex 8.

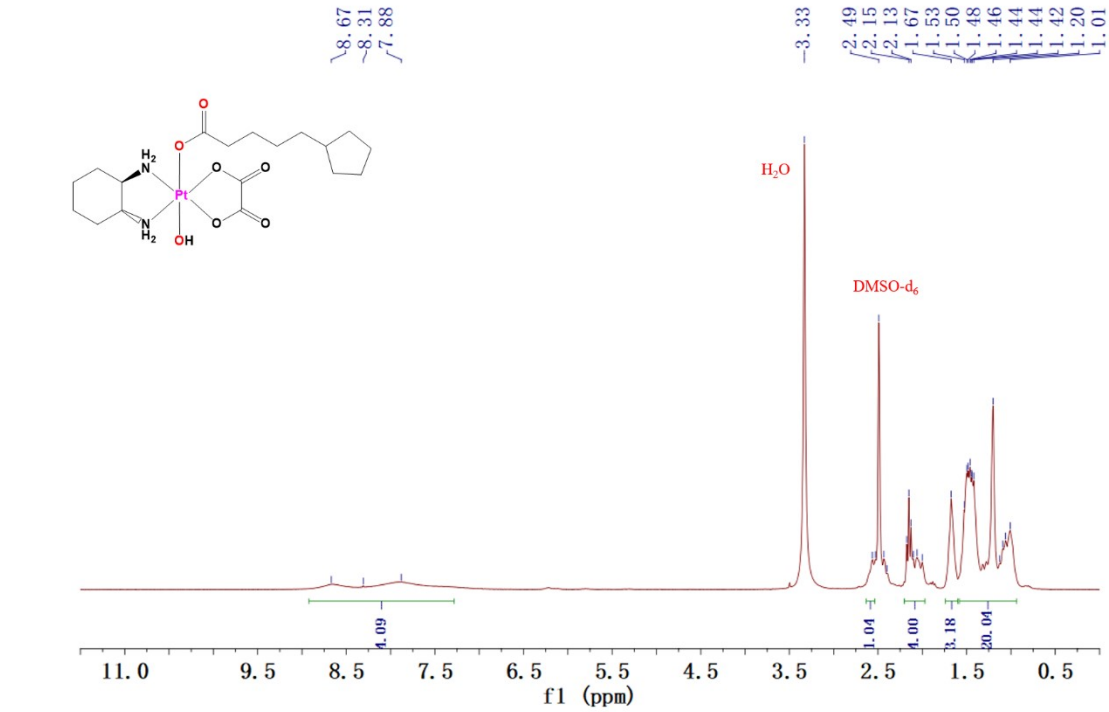

Figure S 45. ^{1}H NMR (400MHz, 297 K, DMSO-d$_6$) spectrum of complex 9.

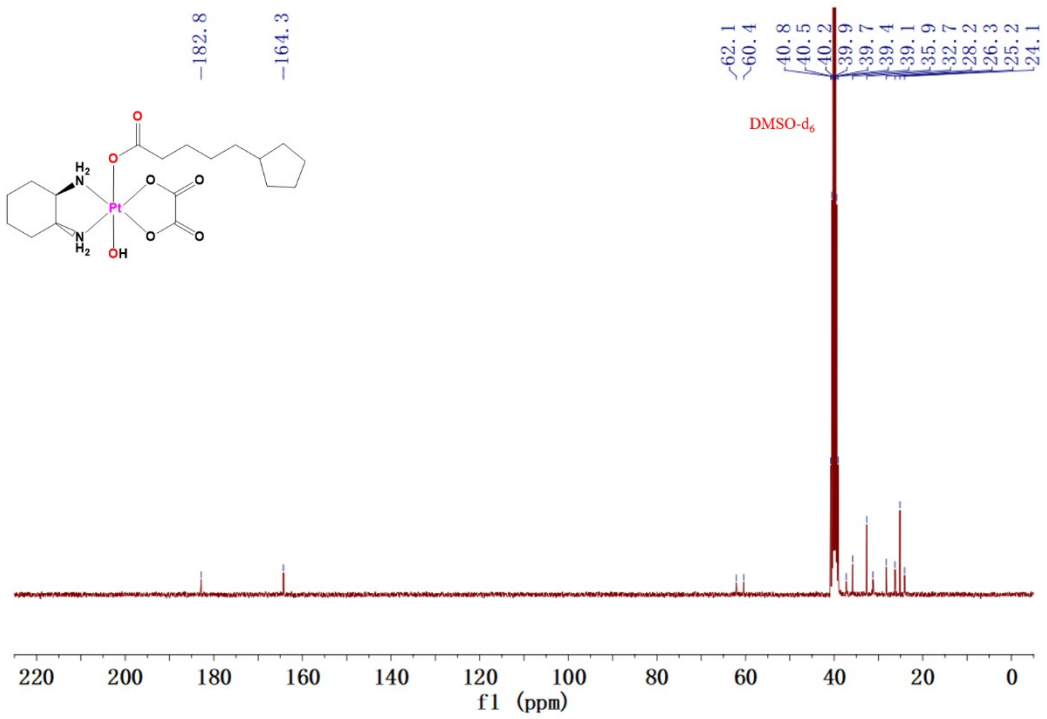

Figure S 46. ^{13}C{^{1}H} NMR (100MHz, 297 K, DMSO-d$_6$) spectrum of complex 9.

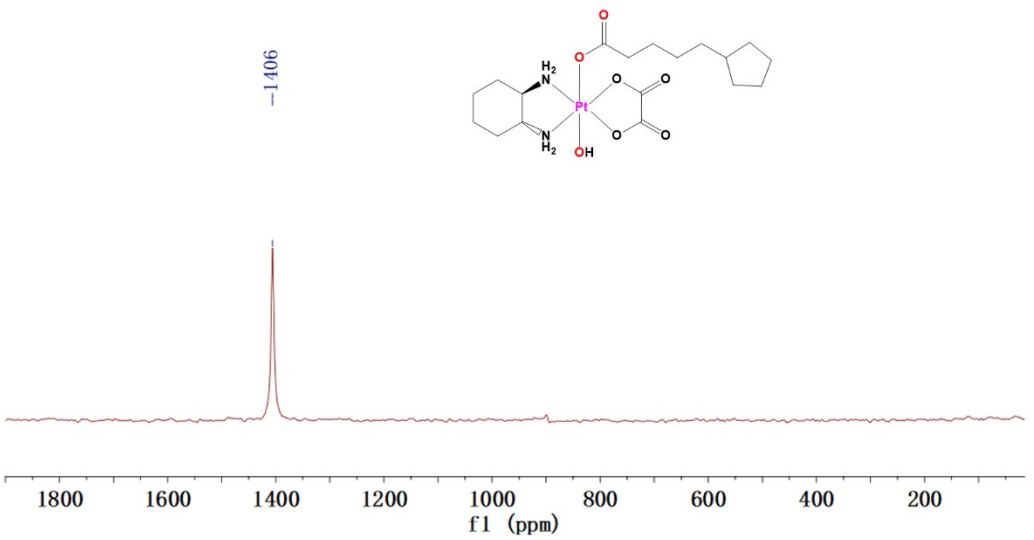

Figure S 47. $^{195}Pt\{^{1}H\}$ NMR (86MHz, 297 K, DMSO-d_6) spectrum of complex 9.

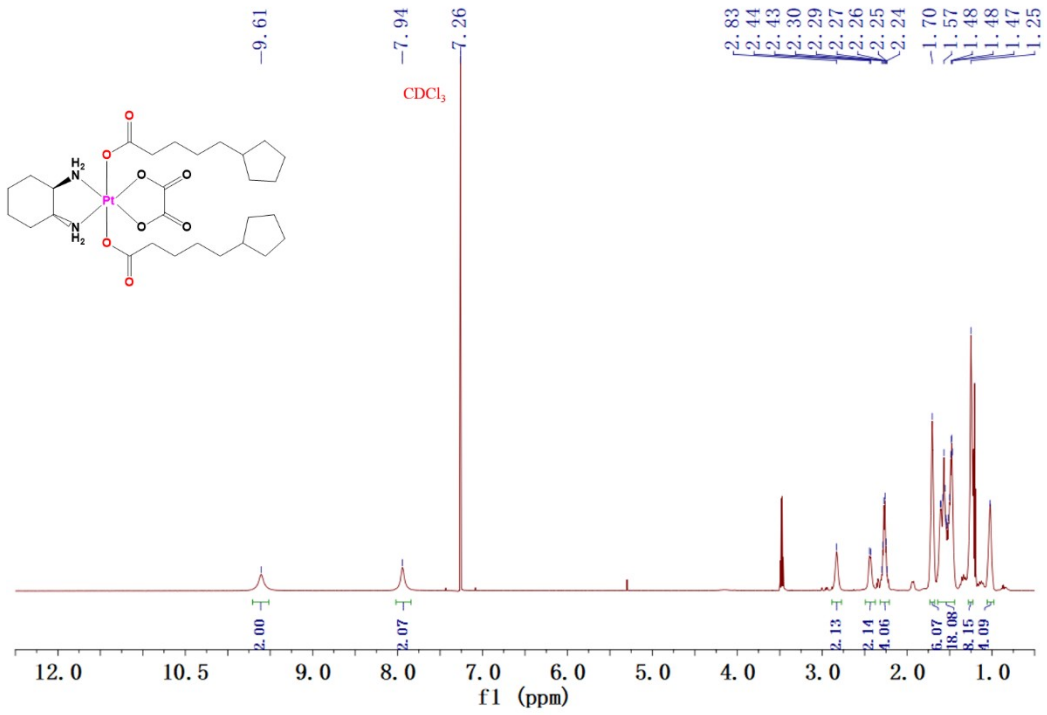

Figure S 48. ^{1}H NMR (400MHz, 297 K, $CDCl_3$) spectrum of complex 10.

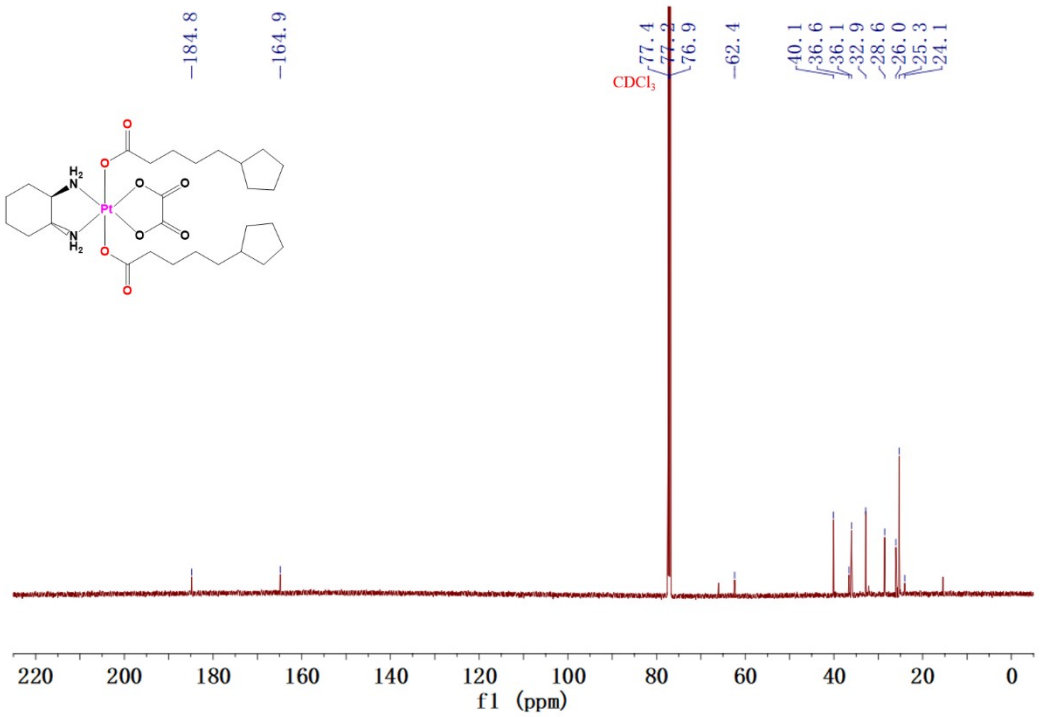

Figure S 49. $^{13}C\{^1H\}$ NMR (100MHz, 297 K, $CDCl_3$) spectrum of complex 10.

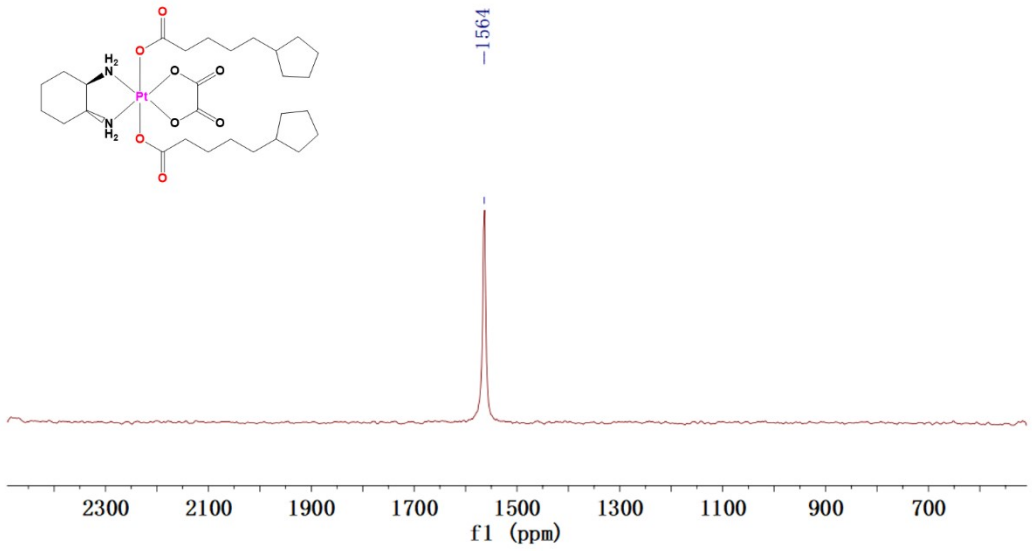

Figure S 50. $^{195}Pt\{^1H\}$ NMR (86MHz, 297 K, $CDCl_3$) spectrum of complex 10.

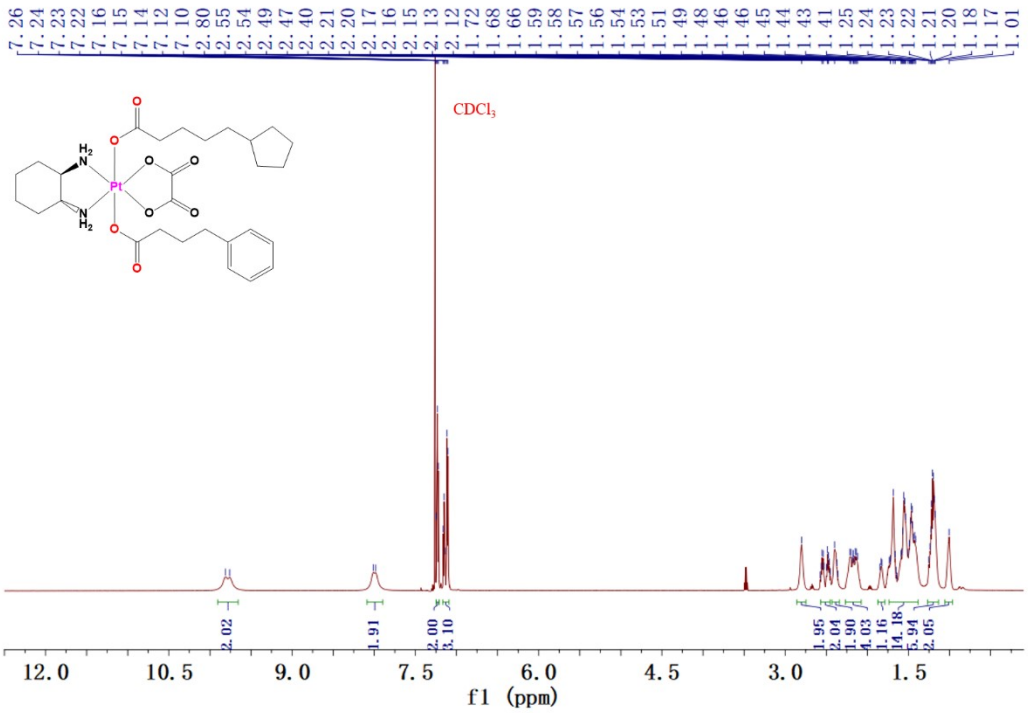

Figure S 51. ^{1}H NMR (400MHz, 297 K, $CDCl_3$) spectrum of complex 11.

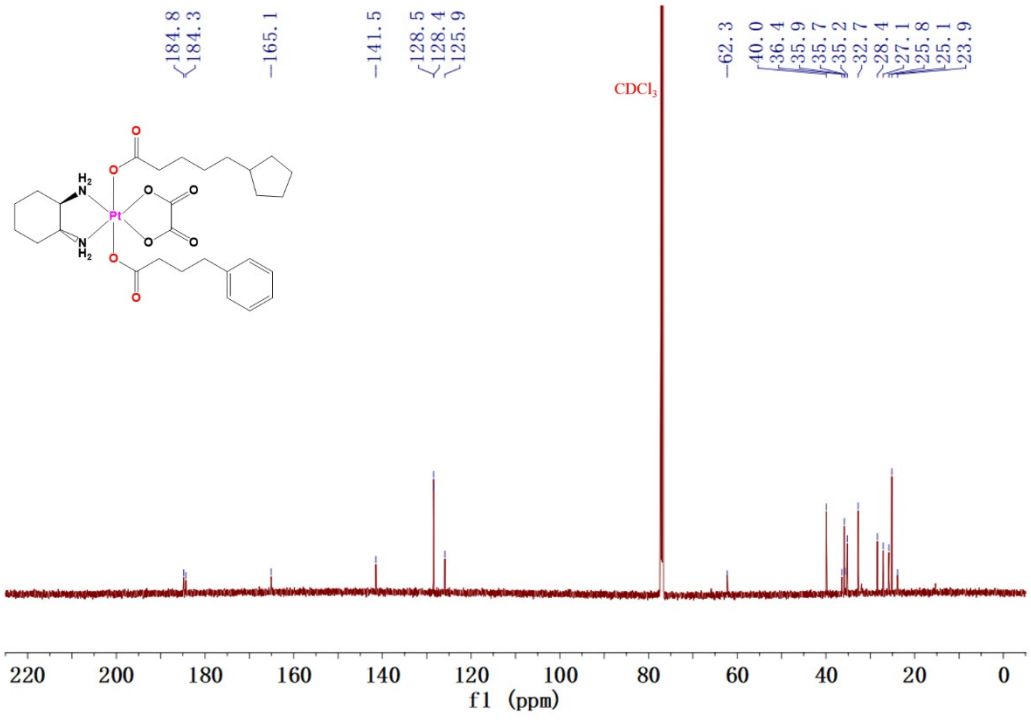

Figure S 52. $^{13}C\{^{1}H\}$ NMR (100MHz, 297 K, $CDCl_3$) spectrum of complex 11.

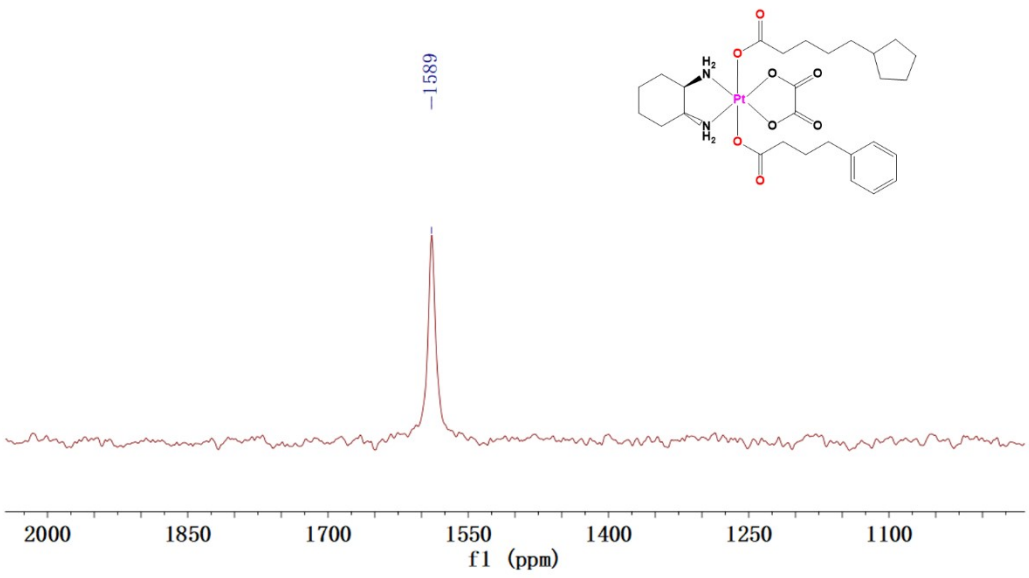

Figure S 53. $^{195}Pt\{^{1}H\}$ NMR (86MHz, 297 K, $CDCl_3$) spectrum of complex 11.

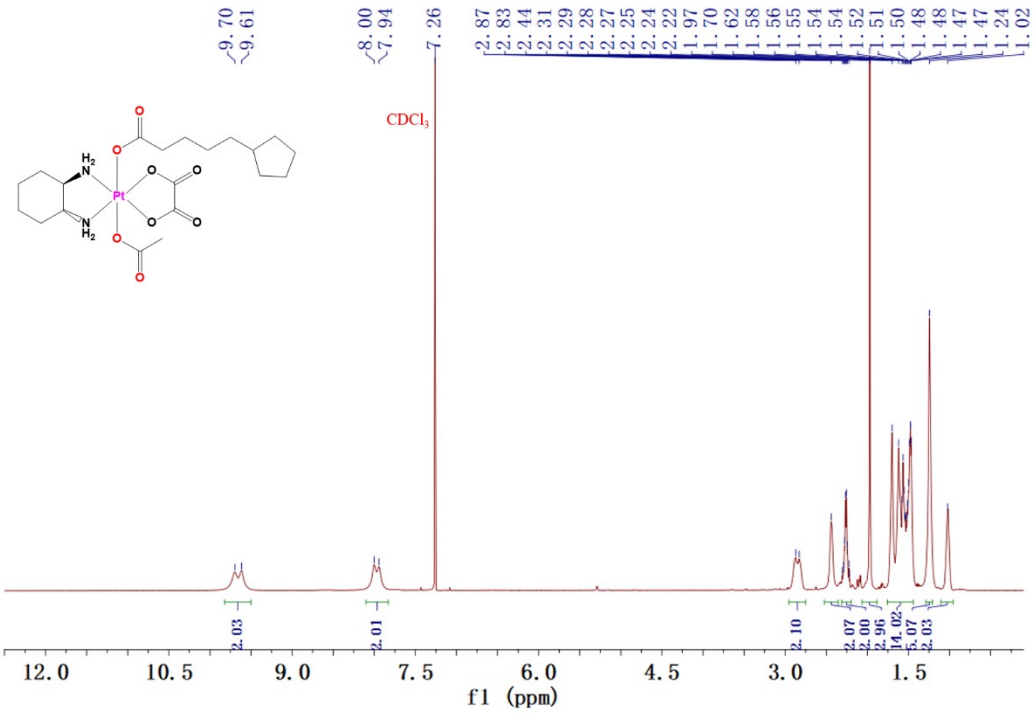

Figure S 54. ^{1}H NMR (600MHz, 297 K, $CDCl_3$) spectrum of complex 12.

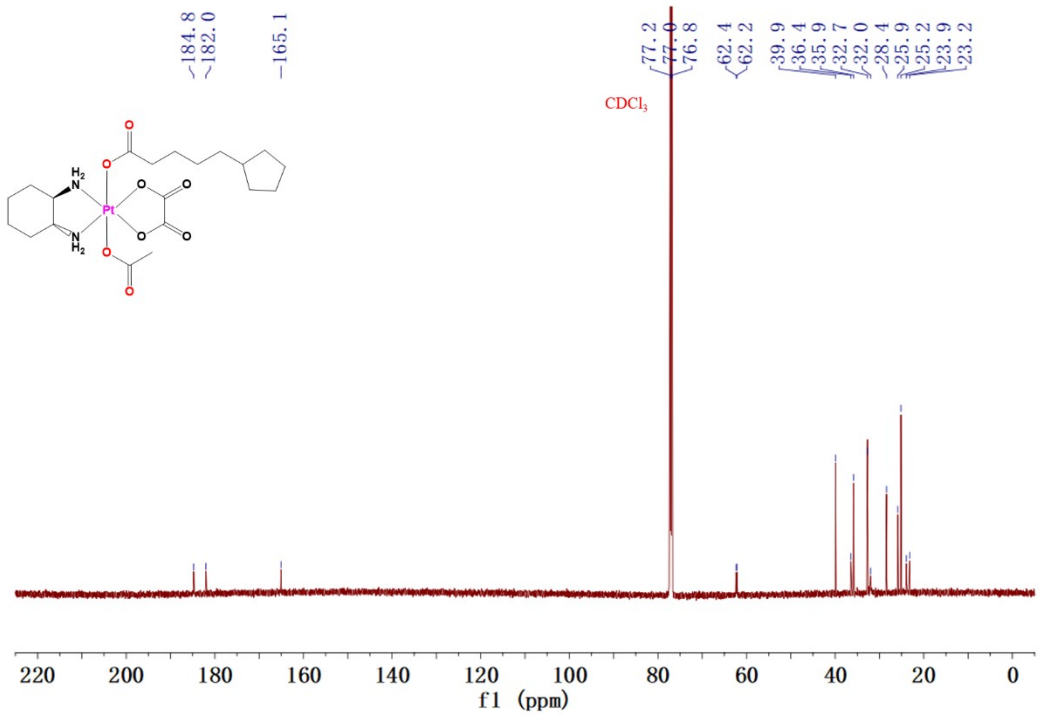

Figure S 55. $^{13}C\{^{1}H\}$ NMR (150MHz, 297 K, $CDCl_3$) spectrum of complex 12.

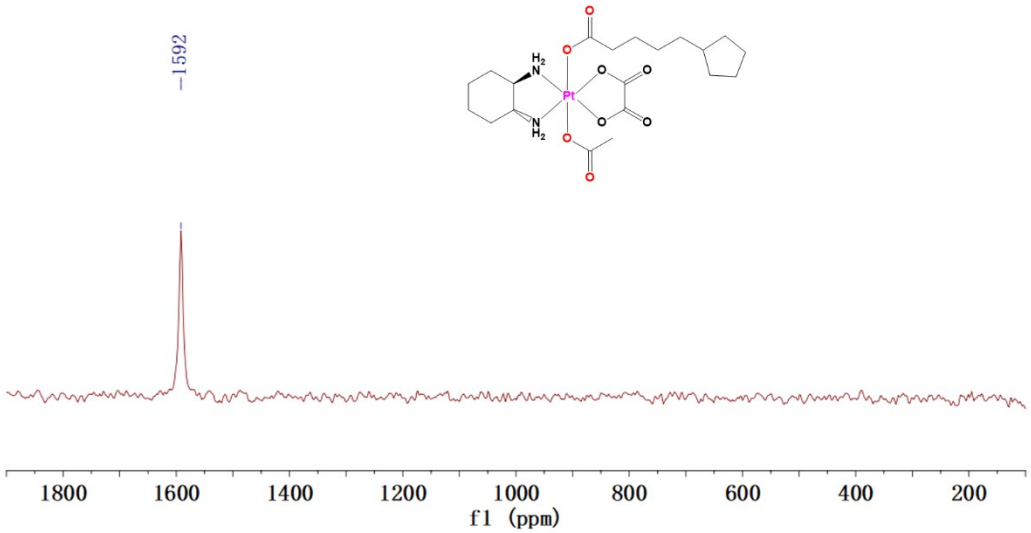

Figure S 56. $^{195}Pt\{^{1}H\}$ NMR (86MHz, 297 K, $CDCl_3$) spectrum of complex 12.

Part 3. MS spectra

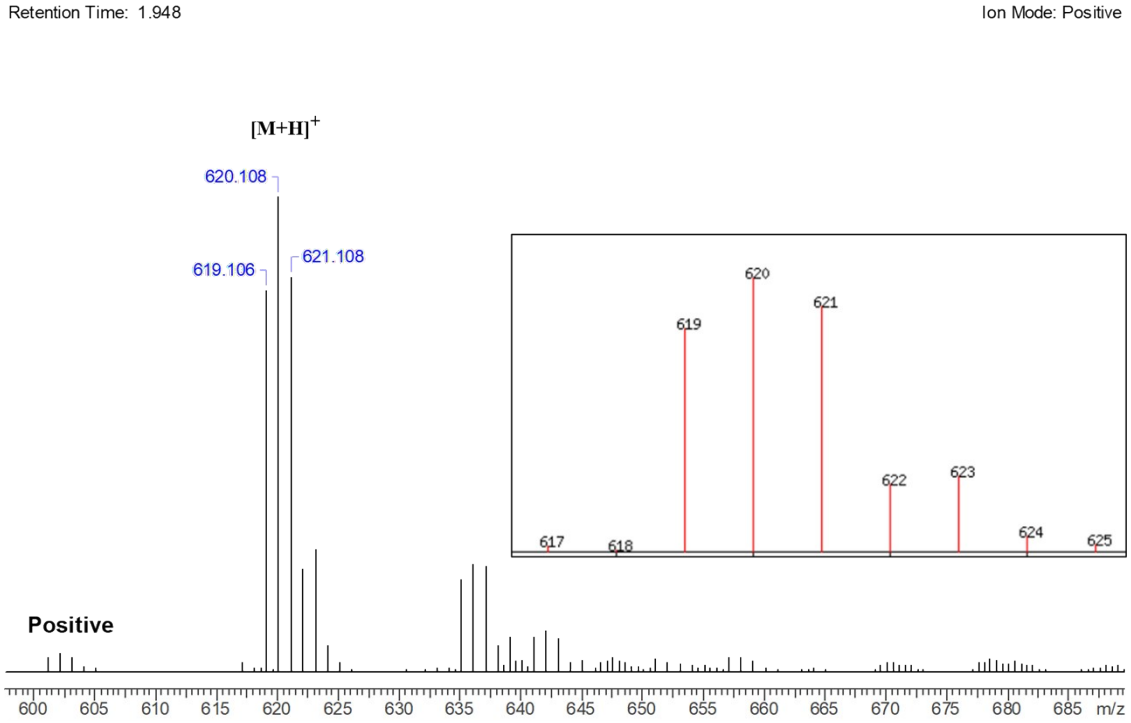

Figure S 57. ESI (+)-MS spectrum of complex 1. The insets show the theoretical isotope patterns $[M+H]^+$.

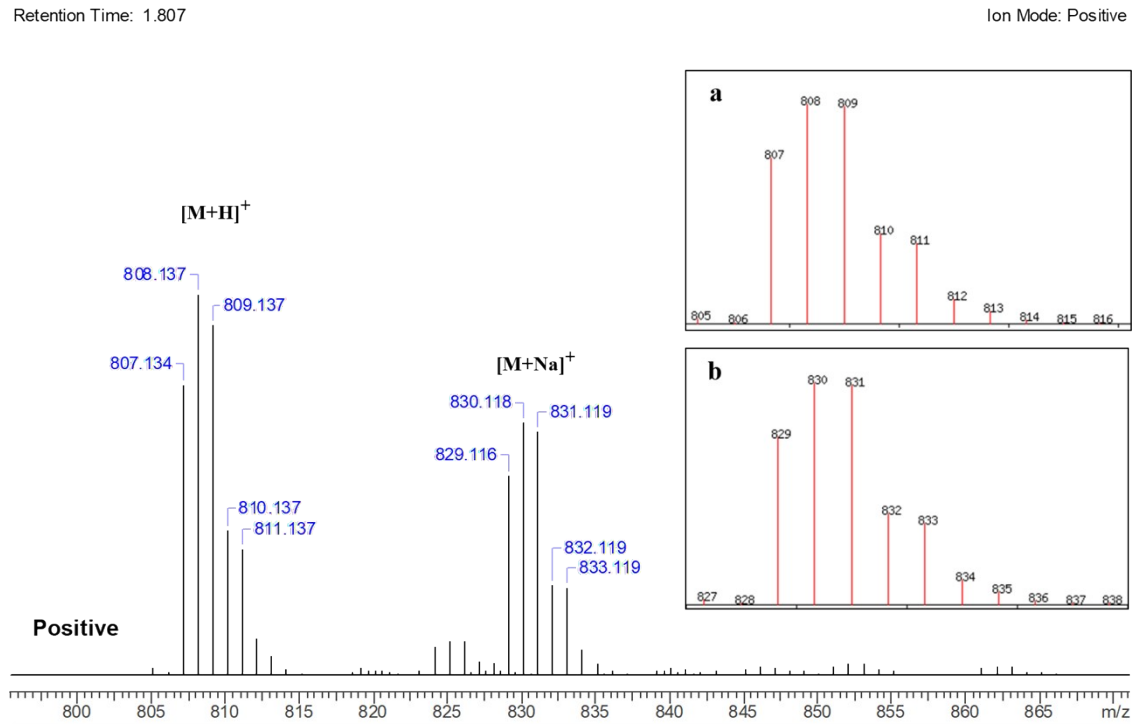

Figure S 58. ESI (+)-MS spectrum of complex 2. The insets show the theoretical isotope patterns (a) $[M+H]^+$ and (b) $[M+Na]^+$.

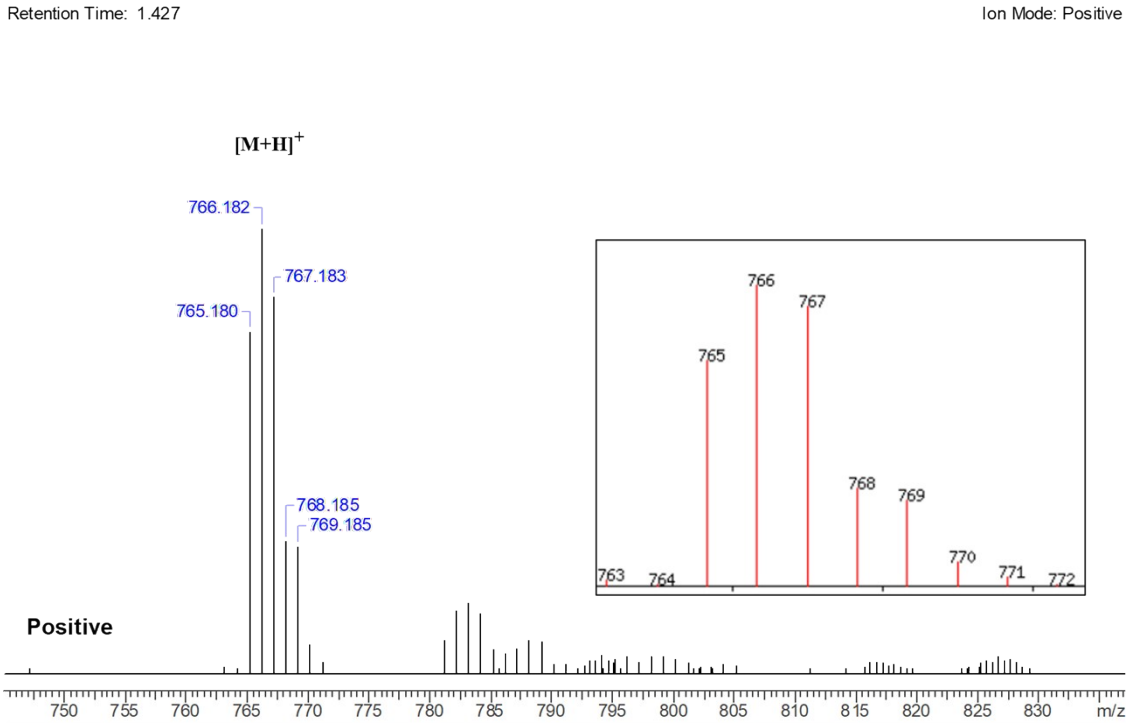

Figure S 59. ESI (+)-MS spectrum of complex 3. The insets show the theoretical isotope patterns $[M+H]^+$.

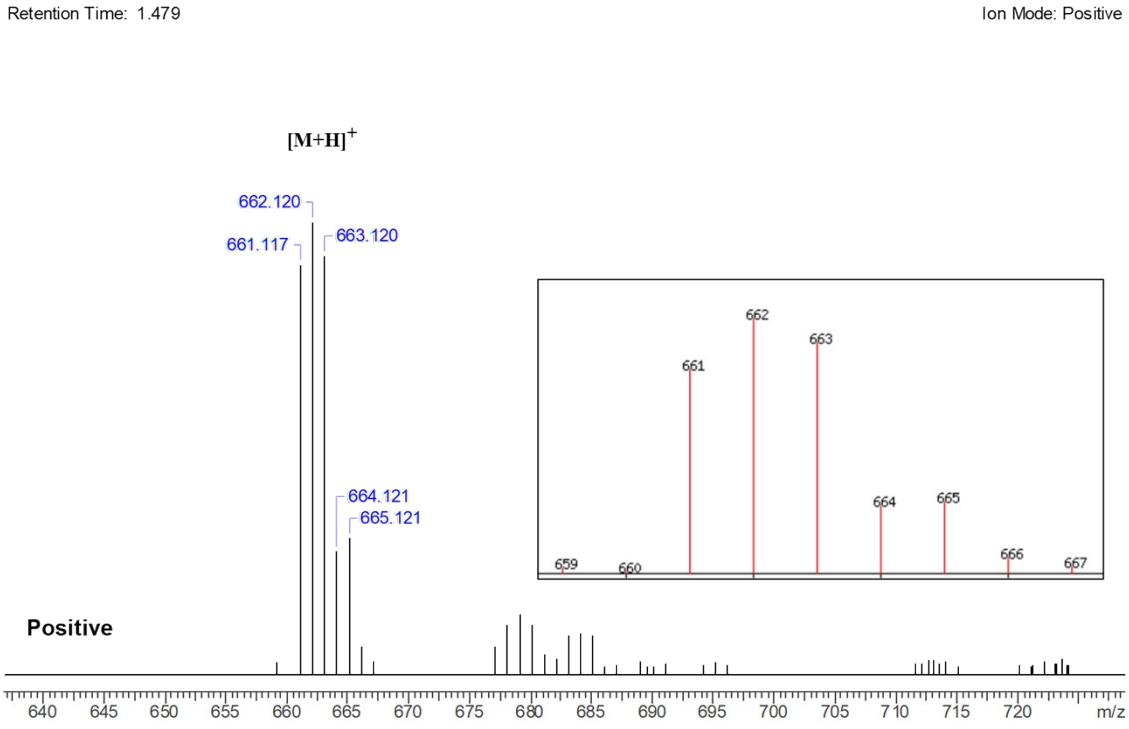

Figure S 60. ESI (+)-MS spectrum of complex 4. The insets show the theoretical isotope patterns $[M+H]^+$.

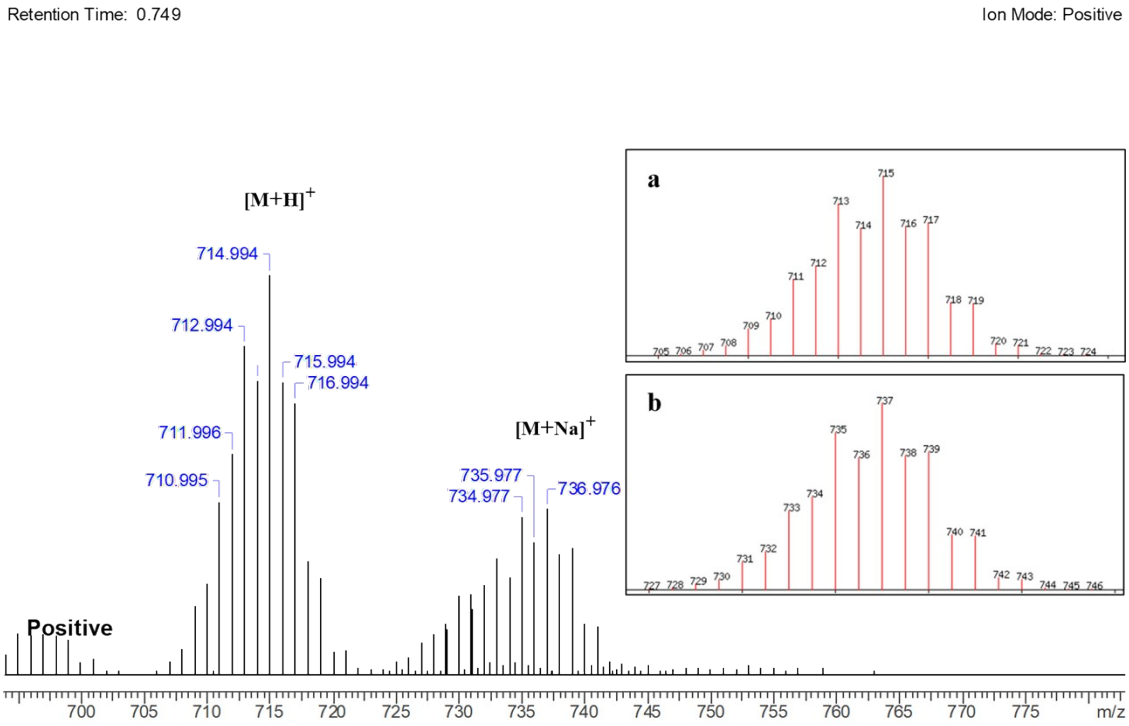

Figure S 61. ESI (+)-MS spectrum of complex 5. The insets show the theoretical isotope patterns (a) $[M+H]^+$ and (b) $[M+Na]^+$.

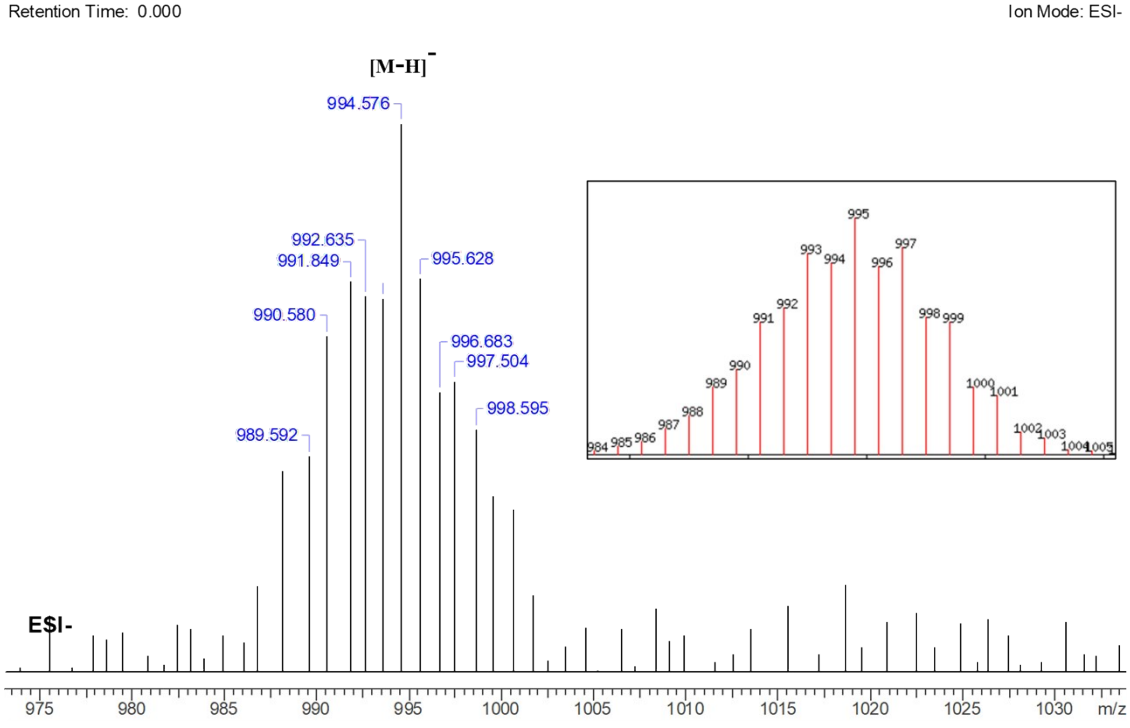

Figure S 62. ESI (-)-MS spectrum of complex 6. The insets show the theoretical isotope patterns $[M-H]^-$.

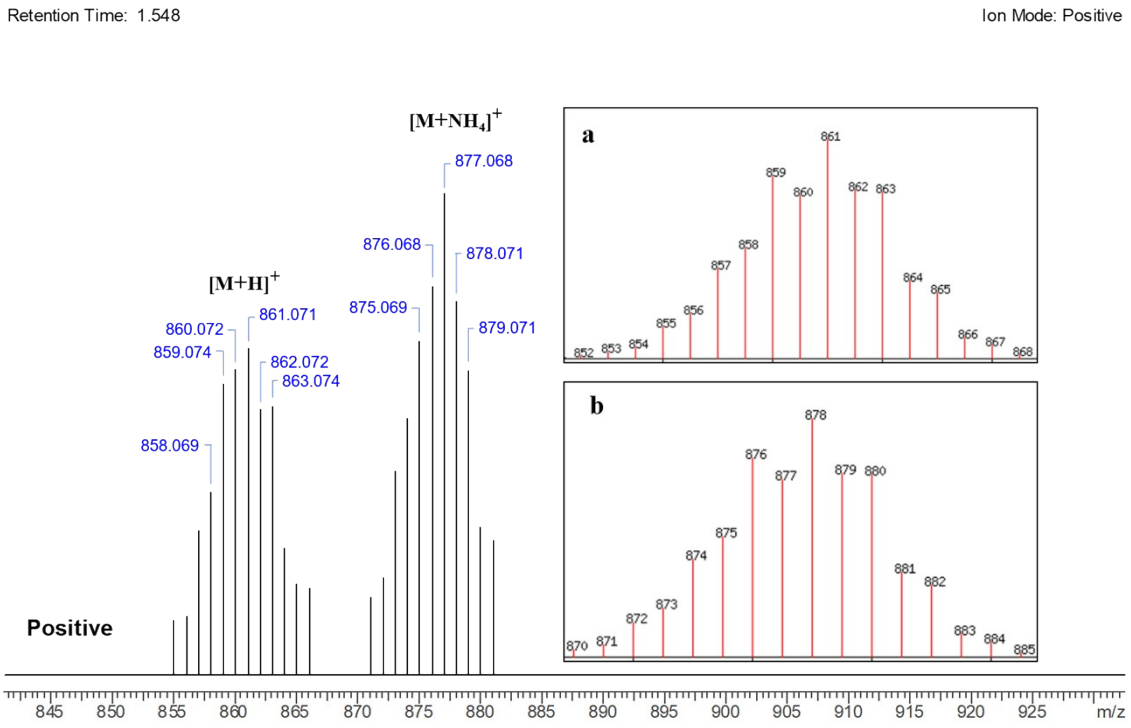

Figure S 63. ESI (+)-MS spectrum of complex 7. The insets show the theoretical isotope patterns (a) $[M+H]^+$ and (b) $[M+NH_4]^+$.

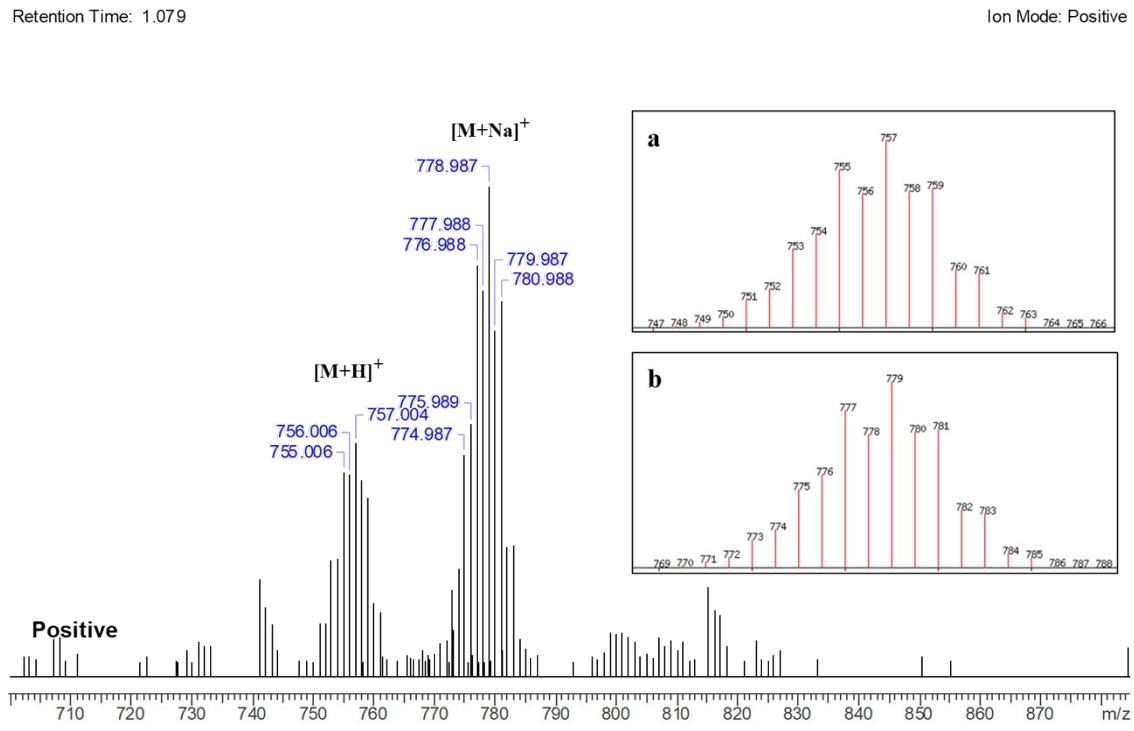

Figure S 64. ESI (+)-MS spectrum of complex 8. The insets show the theoretical isotope patterns (a) $[M+H]^+$ and (b) $[M+Na]^+$.

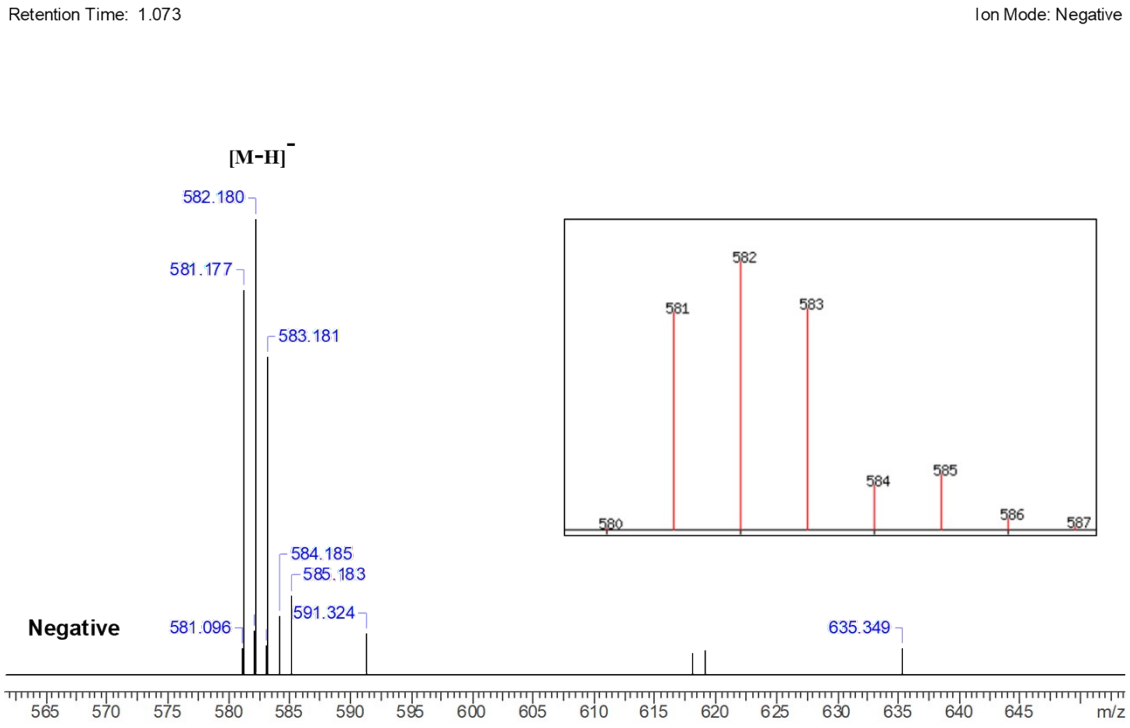

Figure S 65. ESI (-)-MS spectrum of complex 9. The insets show the theoretical isotope patterns [M-H]$^-$.

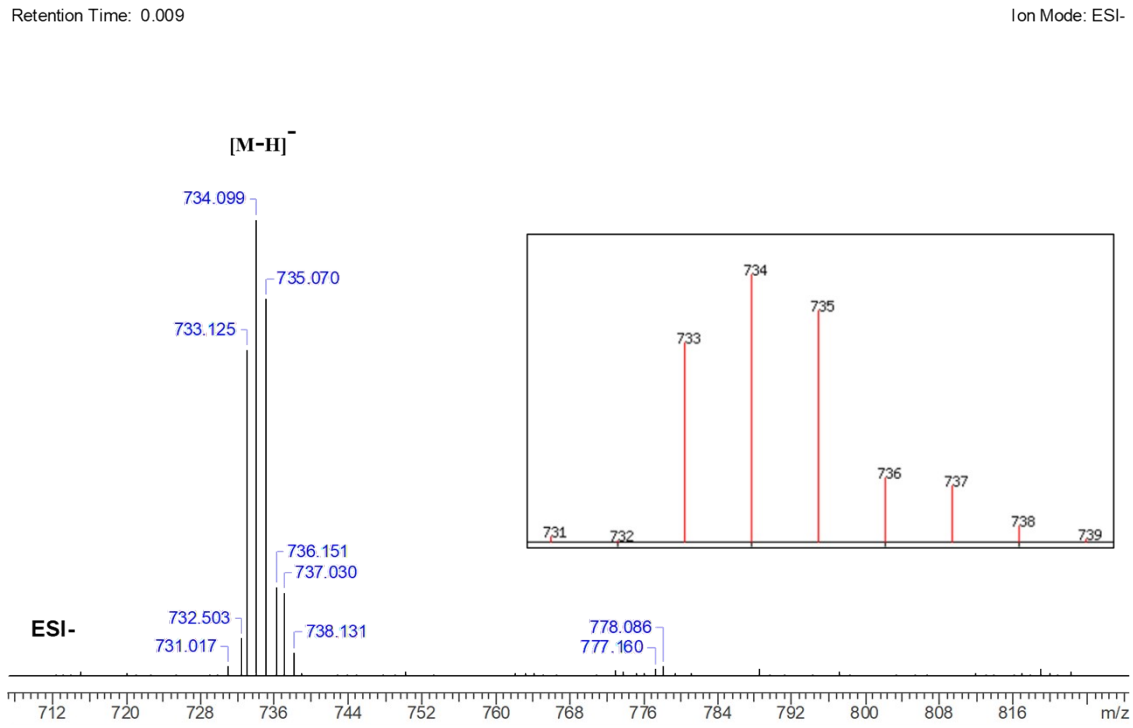

Figure S 66. ESI (-)-MS spectrum of complex 10. The insets show the theoretical isotope patterns [M-H]$^-$.

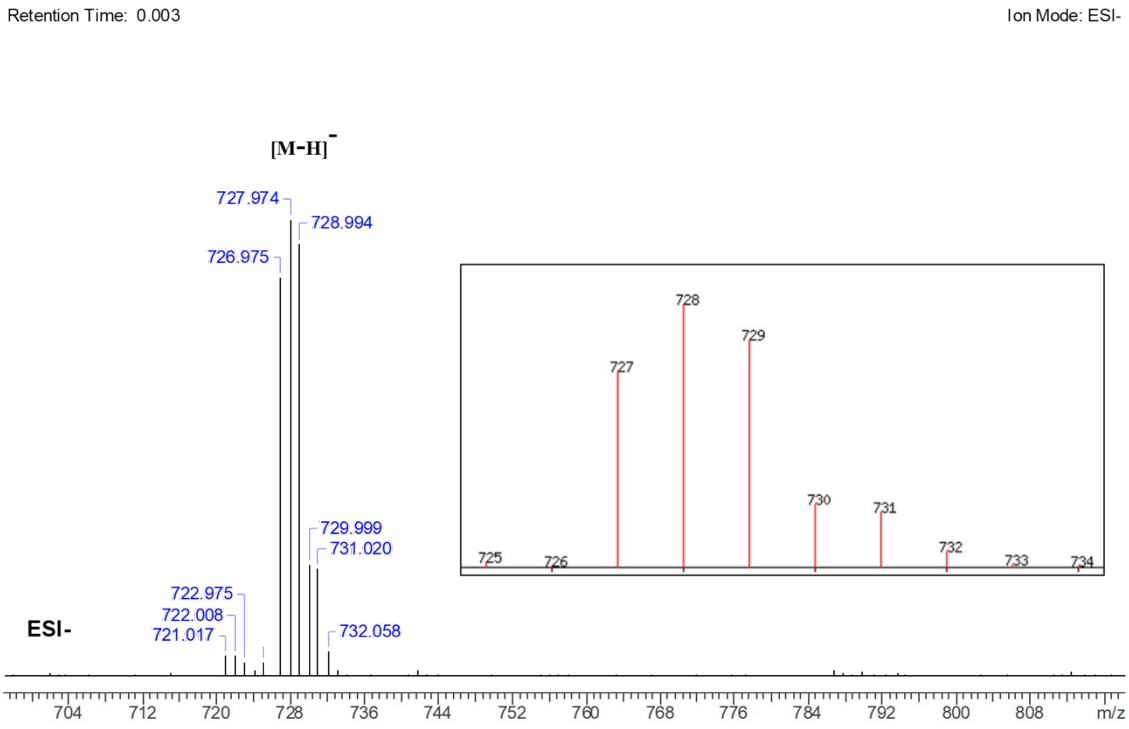

Figure S 67. ESI (-)-MS spectrum of complex 11. The insets show the theoretical isotope patterns $[M-H]^-$.

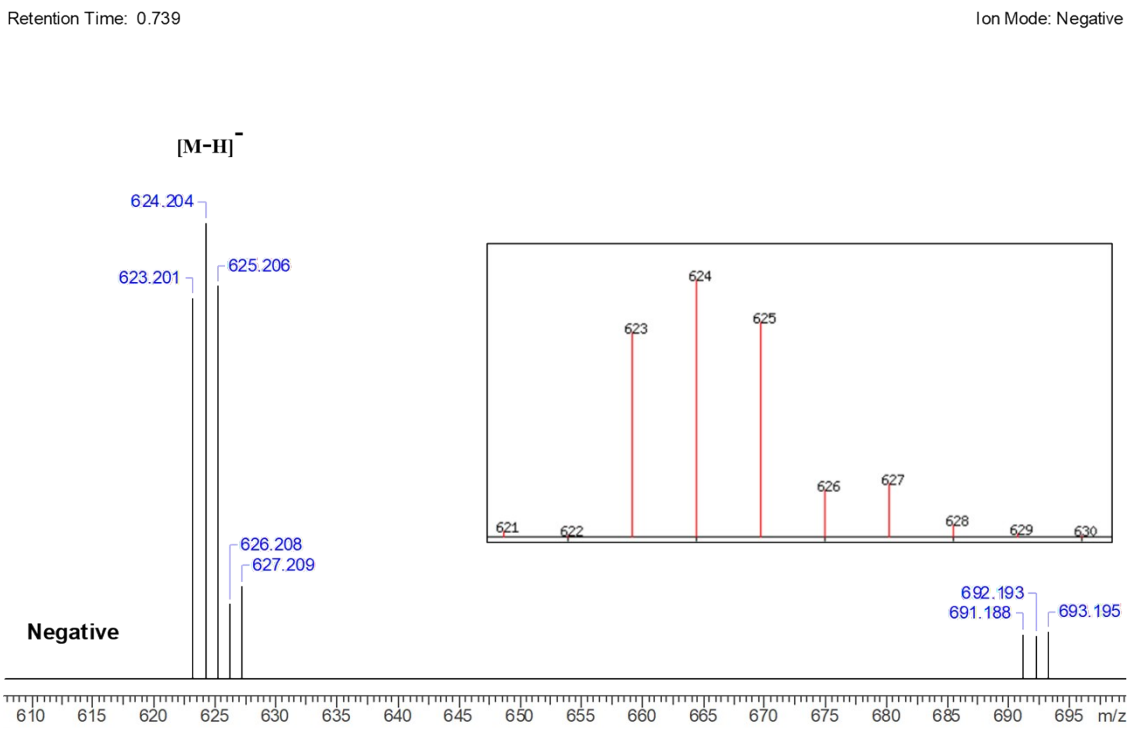

Figure S 68. ESI (-)-MS spectrum of complex 12. The insets show the theoretical isotope patterns $[M-H]^-$.

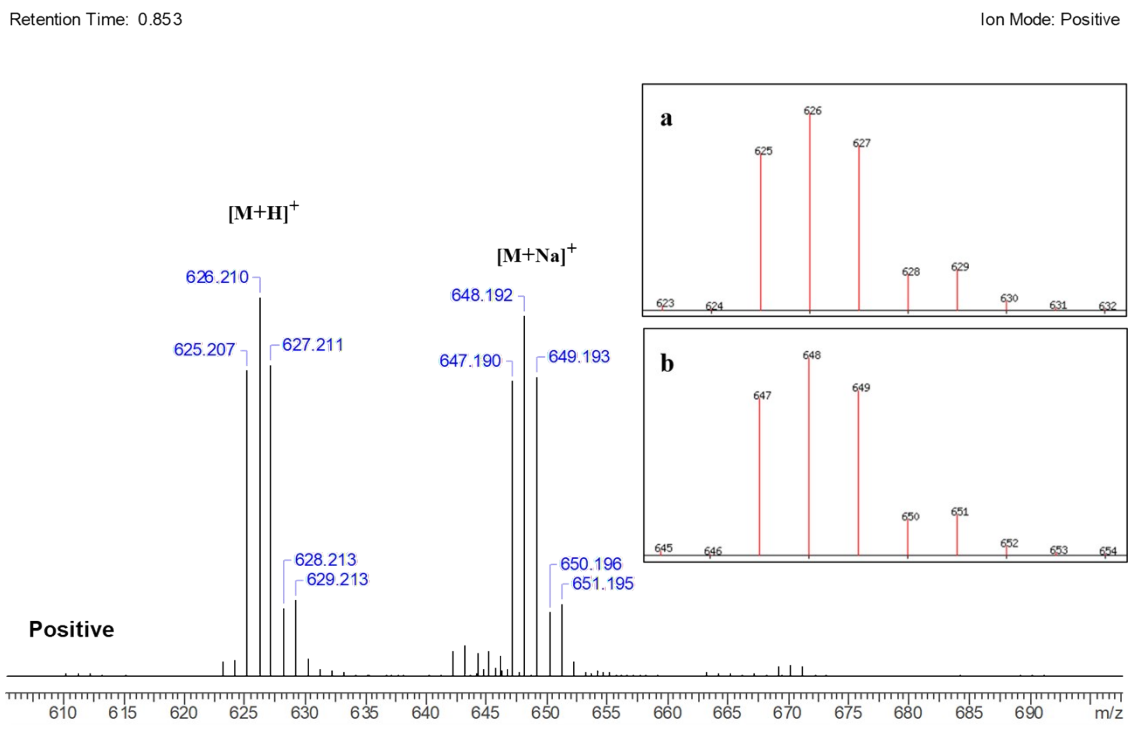

Figure S 69. ESI (+)-MS spectrum of complex 12. The insets show the theoretical isotope patterns (a) $[M+H]^+$ and (b) $[M+Na]^+$.

Part 4. Concentration–effect curves

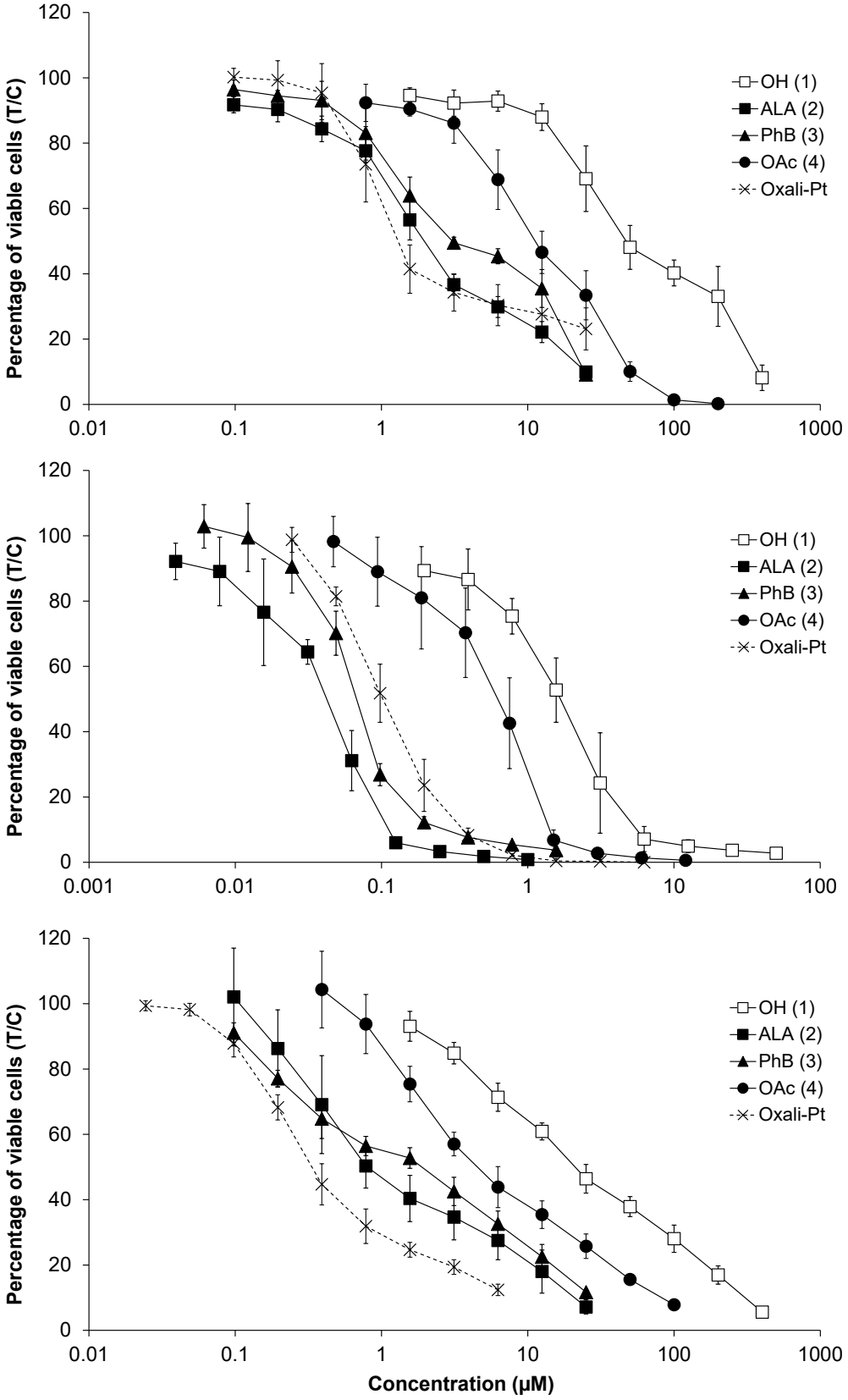

Figure S 70. Concentration–effect curves of oxaPt(ALA)(L) complexes (denoted by the varied ligand L in the legend) in comparison to oxaliplatin in A549 (top), CH1/PA-1 (middle) and SW480 (bottom) cells, based on 96-h MTT assays.

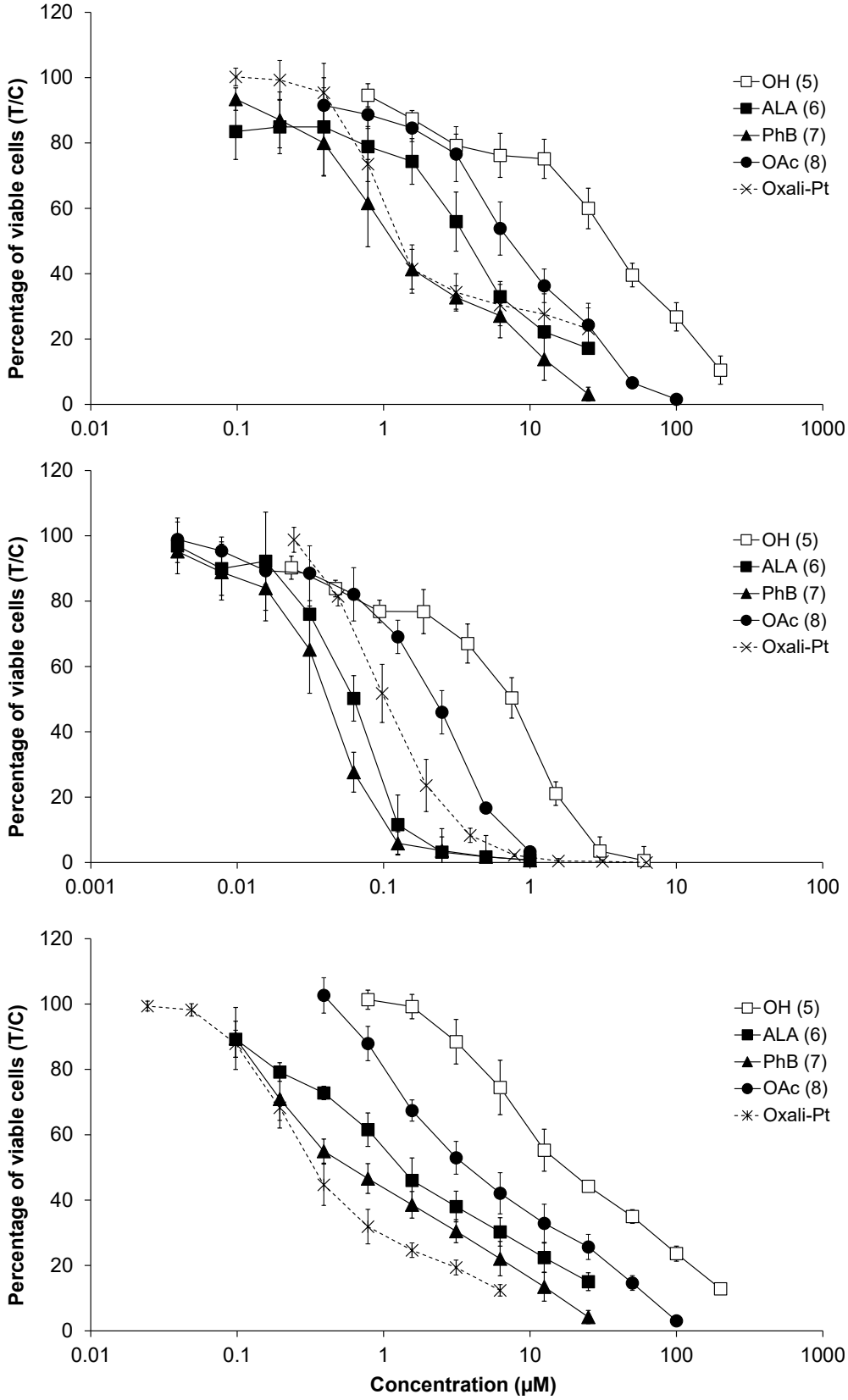

Figure S 71. Concentration–effect curves of oxaPt(SeA)(L) complexes (denoted by the varied ligand L in the legend) in comparison to oxaliplatin in A549 (top), CH1/PA-1 (middle) and SW480 (bottom) cells, based on 96-h MTT assays.

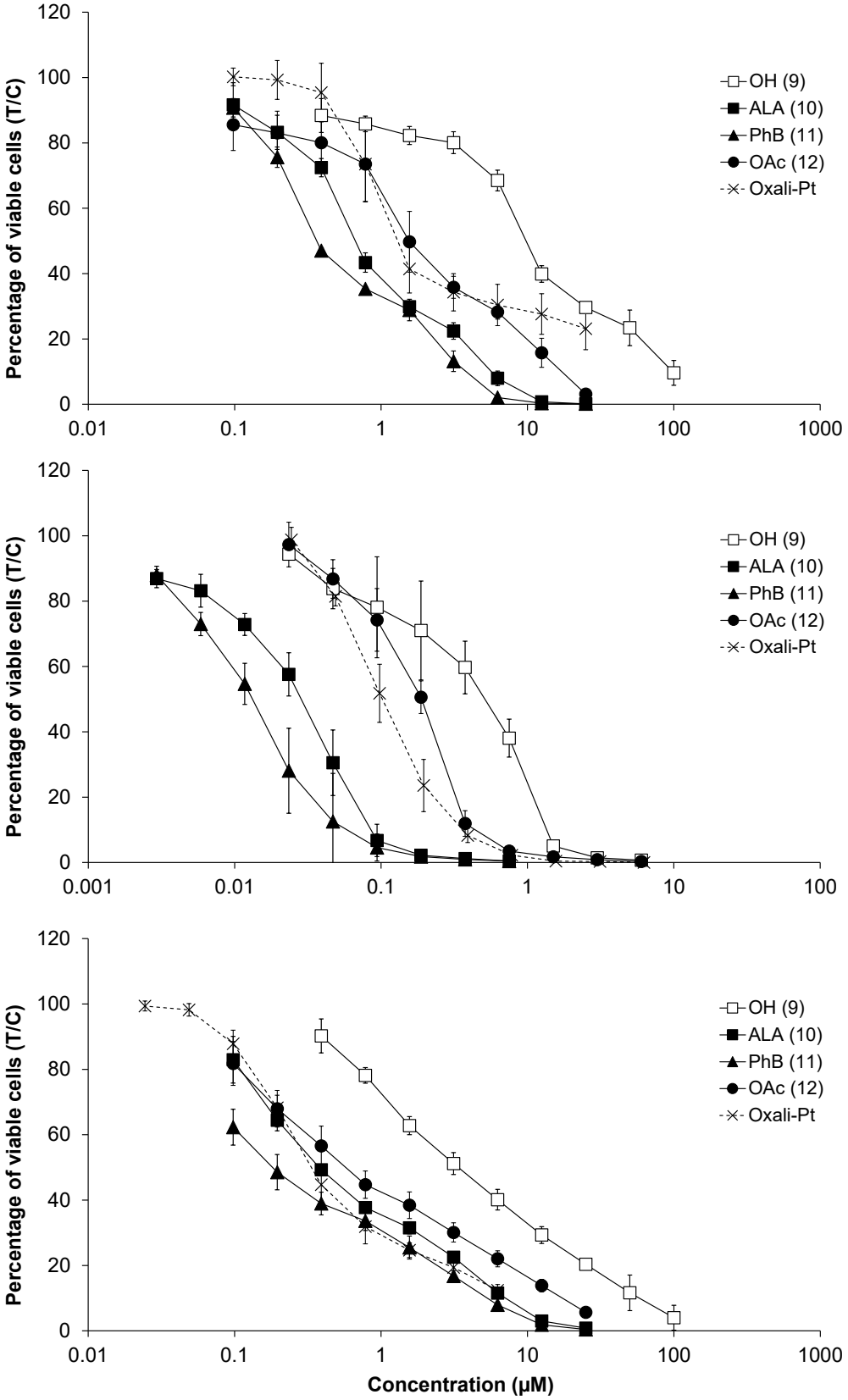

Figure S 72. Concentration–effect curves of oxaPt(CpA)(L) complexes (denoted by the varied ligand L in the legend) in comparison to oxaliplatin in A549 (top), CH1/PA-1 (middle) and SW480 (bottom) cells, based on 96-h MTT assays.